located in the receptor-binding globular head domain (Table 4). As expected, IC-H with S546G, but not the other mutant H proteins, supported cell-to-cell fusion in Vero cells (Fig. 7B). Instead, IC-H with S546G showed a reduced fusion-helper function in H358 and II-18 cells (Fig. 7B). No significant changes were observed in CHO/hSLAM and CV1/hSLAM cells after the introduction of the S546G substitution (Fig. 7B). Similarly, IC-H with L482F showed a reduced fusion-helper function in H358 and II-18 cells but showed activities similar to those seen with IC-H in CHO/hSLAM and CV1/hSLAM cells (Fig. 7B). Quantified and statistical analyses of cell-to-cell fusion in II-18 cells indicated that the areas of syncytia produced by IC-H(S546G) and IC-H(L482F) were significantly smaller than those produced by IC-H ($P < 0.01$) (Fig. 7C). None of the N390M, F555L, and I564L substitutions significantly affected the fusion-helper function in H358 and II-18 cells (Fig. 7B and C). These findings suggested that the L482F and S546G substitutions compromised the ability of the H protein to interact with ECR. It was also noted that the H protein with F555L showed a reduction in the fusion-helper function in CHO/hSLAM and CV1/hSLAM cells (Fig. 7B and C).

DISCUSSION

SLAM is expressed on cells of the immune system and functions as the principal receptor for MV infection (69). However, this molecule probably plays a minor role in MV growth in the CNS, because neural cells in the brain do not express SLAM (28). Indeed, the ability of the SI strain to use SLAM was compromised by the F555L substitution. We and another group recently demonstrated that certain epithelial cells that form tight junctions are highly susceptible to MV infection (25, 50, 59). These data demonstrated the existence of ECR on some epithelial cells (25, 50, 59). ECR probably contributes to the efficient transmission of MV from a patient to other individuals (53), but its roles in persistent infection of the brain with MV remain to be elucidated. ECR is a candidate for an MV receptor in the brain. However, our data indicated that the SI strain had mutated via the S546G and L482F substitutions to use ECR inefficiently. With these data, the idea that ECR functions as a receptor for MV in the brain seemed unconvincing. Instead, the SI-H protein had adapted to use CD46 via the S546G substitution. Woelk et al. identified several positive-selection amino acid sites in the SSPE strain (67), but S546G was absent from the list. It is possible that the S546G substitution was introduced into the SI strain genome during the propagation in Vero cells but not in the brain, since the SI strain was isolated using Vero cells (29). Vero cells are 100 to 1,000 times less sensitive than SLAM-positive B95a cells for the isolation of wt MV strains (22, 34), and wt MV strains readily adapt to use CD46 after several passages in Vero cells (69). However, Ogura et al. (34) indicated that Vero cells were more sensitive than B95a cells for the isolation of SSPE strains. Although their data demonstrated that SSPE strains show cell specificities different from those of wt MV strains, some SSPE strains were shown not to use CD46 as a receptor (47). Nevertheless, it is still possible that the acquisition of the ability to use CD46 contributes to the growth of some SSPE-derived strains in the brain, since various SSPE strains may employ different strategies to acquire the ability to spread in the brain. The SI strain used only CD46 efficiently. Much evidence obtained using CD46-transgenic mice has shown the contributions of CD46 in establishing MV infection of the brain. Analyses using human brain samples also showed that CD46 is a candidate molecule that contributes to the growth of some SSPE strains in the brain (5, 28, 33).

Analyses using animal models have demonstrated that MV uses a transsynaptic route to spread between neurons (24, 27, 35, 40). The data indicated that receptors for the H protein are not required for the transsynaptic transmission (27, 70). It has been suggested that the F protein causes microfusion between neurons without the support of the H protein (27, 70). Ayata et al. (1) demonstrated that the F proteins of some SSPE strains contribute to the exhibition of neurovirulence in animals by showing a hyperfusion activity. Cattaneo et al. (4, 8) also demonstrated that the F proteins of SSPE strains exhibit higher levels of fusion activities than the standard F protein. These data suggest an important role for the F protein in the propagation of SSPE strains in the brain. However, our data indicated that the F protein of the SI strain showed limited membrane fusion activity because of the E300G substitution. It is unlikely that the F protein of the SI strain had acquired the E300G substitution during the propagation in cultured cells, since viruses usually acquire mutations that confer better fitness. Consequently, our data suggest that a high level of membrane fusion activity of the F protein was not a prerequisite for this SSPE strain to spread in the brain. Watanabe et al. (65) suggested that a reduction in cell-to-cell fusion mediated by amino acid changes in the F protein contributes to the persistence of MV in the brain. Their observations are consistent with our data for the SI strain. Thus, the data obtained in the present study provide a clear example of an SSPE-derived strain that exhibits limited fusion activity.

In the present study, we also established a reverse genetics system for the SI strain. Although we previously reported very efficient reverse genetics systems for MV, as shown using recombinant vaccinia viruses encoding T7 RNA polymerase (VV-T7) (30, 55, 56), they were not applicable for rescue of the SI strain from cloned cDNAs. When the previous systems were used (30, 56), infectious cycles of rSI-AcGFP were efficiently initiated in CHO/hSLAM cells by the use of the full-length genome plasmid (data not shown). However, since rSI-AcGFP did not produce cell-free virus particles and replicated poorly, it was impossible to isolate rSI-AcGFP from VV-T7. We tried to use a VV-T7-free system reported by Radecke et al. (39), but neither syncytia nor AcGFP fluorescence was detected. Therefore, a new, efficient VV-T7-free system was required for the rescue of rSI-AcGFP from cloned cDNAs. We are convinced that this new system used for the SI strain would be applicable for other SSPE strains. The success in establishing a reverse genetics system for an SSPE strain is a significant step toward the elucidation of the molecular bases and pathogenesis of SSPE.

ACKNOWLEDGMENTS

We thank T. A. Sato and T. Seya for providing MAbs and N. Ito and M. Sugiyama for providing the BHK/T7-9 cells. We also thank K. Maenaka and all the members of Department of Virology 3, NIID, Japan, for technical help and suggestions.

This work was supported by grants from the Ministry of Education, Culture, Sports, Science and Technology and the Ministry of Health,

Labor and Welfare of Japan and a grant from The Uehara Memorial Foundation.

REFERENCES

1. **Ayata, M., et al.** 2007. Effect of the alterations in the fusion protein of measles virus isolated from brains of patients with subacute sclerosing panencephalitis on syncytium formation. Virus Res. **130:**260–268.
2. **Baricevic, M., D. Forcic, M. Santak, and R. Mazuran.** 2007. A comparison of complete untranslated regions of measles virus genomes derived from wild-type viruses and SSPE brain tissues. Virus Genes **35:**17–27.
3. **Bellini, W. J., et al.** 2005. Subacute sclerosing panencephalitis: more cases of this fatal disease are prevented by measles immunization than was previously recognized. J. Infect. Dis. **192:**1686–1693.
4. **Billeter, M. A., et al.** 1994. Generation and properties of measles virus mutations typically associated with subacute sclerosing panencephalitis. Ann. N. Y. Acad. Sci. **724:**367–377.
5. **Buchholz, C. J., et al.** 1996. Selective expression of a subset of measles virus receptor-competent CD46 isoforms in human brain. Virology **217:**349–355.
6. **Cathomen, T., et al.** 1998. A matrix-less measles virus is infectious and elicits extensive cell fusion: consequences for propagation in the brain. EMBO J. **17:**3899–3908.
7. **Cathomen, T., H. Y. Naim, and R. Cattaneo.** 1998. Measles viruses with altered envelope protein cytoplasmic tails gain cell fusion competence. J. Virol. **72:**1224–1234.
8. **Cattaneo, R., and J. K. Rose.** 1993. Cell fusion by the envelope glycoproteins of persistent measles viruses which caused lethal human brain disease. J. Virol. **67:**1493–1502.
9. **Cattaneo, R., et al.** 1988. Biased hypermutation and other genetic changes in defective measles viruses in human brain infections. Cell **55:**255–265.
10. **Cattaneo, R., et al.** 1986. Accumulated measles virus mutations in a case of subacute sclerosing panencephalitis: interrupted matrix protein reading frame and transcription alteration. Virology **154:**97–107.
11. **Cattaneo, R., et al.** 1989. Mutated and hypermutated genes of persistent measles viruses which caused lethal human brain diseases. Virology **173:**415–425.
12. **Griffin, D. E.** 2007. Measles virus, p. 1551–1585. *In* D. M. Knipe et al. (ed.), Fields virology, 5th ed. Lippincott Williams & Wilkins, Philadelphia, PA.
13. **Grosfeld, H., M. G. Hill, and P. L. Collins.** 1995. RNA replication by respiratory syncytial virus (RSV) is directed by the N, P, and L proteins; transcription also occurs under these conditions but requires RSV superinfection for efficient synthesis of full-length mRNA. J. Virol. **69:**5677–5686.
14. **Hall, W. W., and P. W. Choppin.** 1979. Evidence for lack of synthesis of the M polypeptide of measles virus in brain cells in subacute sclerosing panencephalitis. Virology **99:**443–447.
15. **Hall, W. W., and P. W. Choppin.** 1981. Measles-virus proteins in the brain tissue of patients with subacute sclerosing panencephalitis: absence of the M protein. N. Engl. J. Med. **304:**1152–1155.
16. **Hall, W. W., R. A. Lamb, and P. W. Choppin.** 1979. Measles and subacute sclerosing panencephalitis virus proteins: lack of antibodies to the M protein in patients with subacute sclerosing panencephalitis. Proc. Natl. Acad. Sci. U. S. A. **76:**2047–2051.
17. **Halsey, N. A., et al.** 1980. Risk factors in subacute sclerosing panencephalitis: a case-control study. Am. J. Epidemiol. **111:**415–424.
18. **Hirano, A., A. H. Wang, A. F. Gombart, and T. C. Wong.** 1992. The matrix proteins of neurovirulent subacute sclerosing panencephalitis virus and its acute measles virus progenitor are functionally different. Proc. Natl. Acad. Sci. U. S. A. **89:**8745–8749.
19. **Ishida, H., et al.** 2004. Infection of different cell lines of neural origin with subacute sclerosing panencephalitis (SSPE) virus. Microbiol. Immunol. **48:** 277–287.
20. **Ito, N., et al.** 2003. Improved recovery of rabies virus from cloned cDNA using a vaccinia virus-free reverse genetics system. Microbiol. Immunol. **47:**613–617.
21. **Kato, A., et al.** 1996. Initiation of Sendai virus multiplication from transfected cDNA or RNA with negative or positive sense. Genes Cells **1:**569–579.
22. **Kobune, F., H. Sakata, and A. Sugiura.** 1990. Marmoset lymphoblastoid cells as a sensitive host for isolation of measles virus. J. Virol. **64:**700–705.
23. **Komase, K., et al.** 2006. The phosphoprotein of attenuated measles AIK-C vaccine strain contributes to its temperature-sensitive phenotype. Vaccine **24:**826–834.
24. **Lawrence, D. M., et al.** 2000. Measles virus spread between neurons requires cell contact but not CD46 expression, syncytium formation, or extracellular virus production. J. Virol. **74:**1908–1918.
25. **Leonard, V. H., et al.** 2008. Measles virus blind to its epithelial cell receptor remains virulent in rhesus monkeys but cannot cross the airway epithelium and is not shed. J. Clin. Invest. **118:**2448–2458.
26. **Leyrer, S., W. J. Neubert, and R. Sedlmeier.** 1998. Rapid and efficient recovery of Sendai virus from cDNA: factors influencing recombinant virus rescue. J. Virol. Methods **75:**47–58.
27. **Makhortova, N. R., et al.** 2007. Neurokinin-1 enables measles virus trans-synaptic spread in neurons. Virology **362:**235–244.
28. **McQuaid, S., and S. L. Cosby.** 2002. An immunohistochemical study of the distribution of the measles virus receptors, CD46 and SLAM, in normal human tissues and subacute sclerosing panencephalitis. Lab. Invest. **82:**403–409.
29. **Mirchamsy, H., et al.** 1978. Isolation and characterization of a defective measles virus from brain biopsies of three patients in Iran with subacute sclerosing panencephalitis. Intervirology **9:**106–118.
30. **Nakatsu, Y., M. Takeda, M. Kidokoro, M. Kohara, and Y. Yanagi.** 2006. Rescue system for measles virus from cloned cDNA driven by vaccinia virus Lister vaccine strain. J. Virol. Methods **137:**152–155.
31. **Ning, X., et al.** 2002. Alterations and diversity in the cytoplasmic tail of the fusion protein of subacute sclerosing panencephalitis virus strains isolated in Osaka, Japan. Virus Res. **86:**123–131.
32. **Niwa, H., K. Yamamura, and J. Miyazaki.** 1991. Efficient selection for high-expression transfectants with a novel eukaryotic vector. Gene **108:**193–199.
33. **Ogata, A., et al.** 1997. Absence of measles virus receptor (CD46) in lesions of subacute sclerosing panencephalitis brains. Acta Neuropathol. **94:**444–449.
34. **Ogura, H., et al.** 1997. Efficient isolation of subacute sclerosing panencephalitis virus from patient brains by reference to magnetic resonance and computed tomographic images. J. Neurovirol. **3:**304–309.
35. **Oldstone, M. B. A., et al.** 1999. Measles virus infection in a transgenic model: virus-induced immunosuppression and central nervous system disease. Cell **98:**629–640.
36. **Ono, N., et al.** 2001. Measles viruses on throat swabs from measles patients use signaling lymphocytic activation molecule (CDw150) but not CD46 as a cellular receptor. J. Virol. **75:**4399–4401.
37. **Parks, C. L., et al.** 2001. Comparison of predicted amino acid sequences of measles virus strains in the Edmonston vaccine lineage. J. Virol. **75:**910–920.
38. **Radecke, F., and M. A. Billeter.** 1995. Appendix: measles virus antigenome and protein consensus sequences. Curr. Top. Microbiol. Immunol. **191:**181–192.
39. **Radecke, F., et al.** 1995. Rescue of measles viruses from cloned DNA. EMBO J. **14:**5773–5784.
40. **Rall, G. F., et al.** 1997. A transgenic mouse model for measles virus infection of the brain. Proc. Natl. Acad. Sci. U. S. A. **94:**4659–4663.
41. **Richardson, C. D., A. Scheid, and P. W. Choppin.** 1980. Specific inhibition of paramyxovirus and myxovirus replication by oligopeptides with amino acid sequences similar to those at the N-termini of the F1 or HA2 viral polypeptides. Virology **105:**205–222.
42. **Sato, T. A., A. Fukuda, and A. Sugiura.** 1985. Characterization of major structural proteins of measles virus with monoclonal antibodies. J. Gen. Virol. **66:**1397–1409.
43. **Sato, T. A., M. Hayami, and K. Yamanouchi.** 1981. Antibody response to structural proteins of measles virus in patients with natural measles and subacute sclerosing panencephalitis. Jpn. J. Med. Sci. Biol. **34:**365–373.
44. **Schmid, A., et al.** 1992. Subacute sclerosing panencephalitis is typically characterized by alterations in the fusion protein cytoplasmic domain of the persisting measles virus. Virology **188:**910–915.
45. **Seki, F., M. Takeda, H. Minagawa, and Y. Yanagi.** 2006. Recombinant wild-type measles virus containing a single N481Y substitution in its haemagglutinin cannot use receptor CD46 as efficiently as that having the haemagglutinin of the Edmonston laboratory strain. J. Gen. Virol. **87:**1643–1648.
46. **Seya, T., et al.** 1995. Blocking measles virus infection with a recombinant soluble from of, or monoclonal antibodies against, membrane cofactor protein of complement (CD46). Immunology **84:**619–625.
47. **Shingai, M., et al.** 2003. Receptor use by vesicular stomatitis virus pseudotypes with glycoproteins of defective variants of measles virus isolated from brains of patients with subacute sclerosing panencephalitis. J. Gen. Virol. **84:**2133–2143.
48. **Shirogane, Y., et al.** 2008. Efficient multiplication of human metapneumovirus in Vero cells expressing the transmembrane serine protease TMPRSS2. J. Virol. **82:**8942–8946.
49. **Shirogane, Y., et al.** 2010. Epithelial-mesenchymal transition abolishes the susceptibility of polarized epithelial cell lines to measles virus. J. Biol. Chem. **285:**20882–20890.
50. **Tahara, M., et al.** 2008. Measles virus infects both polarized epithelial and immune cells by using distinctive receptor-binding sites on its hemagglutinin. J. Virol. **82:**4630–4637.
51. **Tahara, M., M. Takeda, and Y. Yanagi.** 2005. Contributions of matrix and large protein genes of the measles virus Edmonston strain to growth in cultured cells as revealed by recombinant viruses. J. Virol. **79:**15218–15225.
52. **Takasu, T., et al.** 2003. A continuing high incidence of subacute sclerosing panencephalitis (SSPE) in the Eastern Highlands of Papua New Guinea. Epidemiol. Infect. **131:**887–898.
53. **Takeda, M.** 2008. Measles virus breaks through epithelial cell barriers to achieve transmission. J. Clin. Invest. **118:**2386–2389.
54. **Takeda, M., et al.** 1998. Measles virus attenuation associated with transcriptional impediment and a few amino acid changes in the polymerase and accessory proteins. J. Virol. **72:**8690–8696.

55. **Takeda, M., et al.** 2006. Generation of measles virus with a segmented RNA genome. J. Virol. **80:**4242–4248.
56. **Takeda, M., et al.** 2005. Efficient rescue of measles virus from cloned cDNA using SLAM-expressing Chinese hamster ovary cells. Virus Res. **108:**161–165.
57. **Takeda, M., et al.** 2005. Long untranslated regions of the measles virus M and F genes control virus replication and cytopathogenicity. J. Virol. **79:** 14346–14354.
58. **Takeda, M., et al.** 2008. Measles viruses possessing the polymerase protein genes of the Edmonston vaccine strain exhibit attenuated gene expression and growth in cultured cells and SLAM knock-in mice. J. Virol. **82:**11979–11984.
59. **Takeda, M., et al.** 2007. A human lung carcinoma cell line supports efficient measles virus growth and syncytium formation via a SLAM- and CD46-independent mechanism. J. Virol. **81:**12091–12096.
60. **Takeda, M., et al.** 2000. Recovery of pathogenic measles virus from cloned cDNA. J. Virol. **74:**6643–6647.
61. **Takeuchi, K., N. Miyajima, F. Kobune, and M. Tashiro.** 2000. Comparative nucleotide sequence analysis of the entire genomes of B95a cell-isolated and Vero cell-isolated measles viruses from the same patient. Virus Genes **20:** 253–257.
62. **Tatsuo, H., N. Ono, K. Tanaka, and Y. Yanagi.** 2000. SLAM (CDw150) is a cellular receptor for measles virus. Nature **406:**893–897.
63. **Thompson, J. D., D. G. Higgins, and T. J. Gibson.** 1994. CLUSTAL W: improving the sensitivity of progressive multiple sequence alignment through sequence weighting, position-specific gap penalties and weight matrix choice. Nucleic Acids Res. **22:**4673–4680.
64. **Wang, D., Y. Zhang, Z. Zhang, J. Zhu, and J. Yu.** 2010. KaKs_Calculator 2.0: a toolkit incorporating gamma-series methods and sliding window strategies. Genomics Proteomics Bioinformatics **8:**77–80.
65. **Watanabe, M., et al.** 1995. Delayed activation of altered fusion glycoprotein in a chronic measles virus variant that causes subacute sclerosing panencephalitis. J. Neurovirol. **1:**177–188.
66. **WHO.** 2003. Update of the nomenclature for describing the genetic characteristics of wild-type measles viruses: new genotypes and reference strains. Wkly. Epidemiol. Rec. **78:**229–232.
67. **Woelk, C. H., O. G. Pybus, L. Jin, D. W. Brown, and E. C. Holmes.** 2002. Increased positive selection pressure in persistent (SSPE) versus acute measles virus infections. J. Gen. Virol. **83:**1419–1430.
68. **Wong, T. C., et al.** 1989. Generalized and localized biased hypermutation affecting the matrix gene of a measles virus strain that causes subacute sclerosing panencephalitis. J. Virol. **63:**5464–5468.
69. **Yanagi, Y., M. Takeda, S. Ohno, and T. Hashiguchi.** 2009. Measles virus receptors. Curr. Top. Microbiol. Immunol. **329:**13–30.
70. **Young, V. A., and G. F. Rall.** 2009. Making it to the synapse: measles virus spread in and among neurons. Curr. Top. Microbiol. Immunol. **330:**3–30.

Biochemical and Biophysical Research Communications 418 (2012) 38–43

Contents lists available at SciVerse ScienceDirect

Biochemical and Biophysical Research Communications

journal homepage: www.elsevier.com/locate/ybbrc

Epitope mapping of neutralizing monoclonal antibody in avian influenza A H5N1 virus hemagglutinin

Takashi Ohkura [a], Yuji Kikuchi [a,b], Naoko Kono [c], Shigeyuki Itamura [c], Katsuhiro Komase [d,e], Fumitaka Momose [a], Yuko Morikawa [a,*]

[a] Graduate School of Infection Control Sciences, Kitasato University, Shirokane 5-9-1, Minato-ku, Tokyo 108-8641, Japan
[b] Faculty of Pharmacy, Iwaki Meisei University, Fukushima 970-8551, Japan
[c] Center for Influenza Virus Research, National Institute of Infectious Diseases, Tokyo 208-0011, Japan
[d] Department of Virology III, National Institute of Infectious Diseases, Tokyo 208-0011, Japan
[e] Research Center for Biologicals, Kitasato Institute, Saitama 364-0026, Japan

ARTICLE INFO

Article history:
Received 19 December 2011
Available online 27 December 2011

Keywords:
Influenza
Vaccine
H5N1
Neutralizing antibody
Epitope
scFv

ABSTRACT

The global spread of highly pathogenic avian influenza A H5N1 viruses raises concerns about more widespread infection in the human population. Pre-pandemic vaccine for H5N1 clade 1 influenza viruses has been produced from the A/Viet Nam/1194/2004 strain (VN1194), but recent prevalent avian H5N1 viruses have been categorized into the clade 2 strains, which are antigenically distinct from the pre-pandemic vaccine. To understand the antigenicity of H5N1 hemagglutinin (HA), we produced a neutralizing monoclonal antibody (mAb12–1G6) using the pre-pandemic vaccine. Analysis with chimeric and point mutant HAs revealed that mAb12–1G6 bound to the loop (amino acid positions 140–145) corresponding to an antigenic site A in the H3 HA. mAb12–1G6 failed to bind to the mutant VN1194 HA when only 3 residues were substituted with the corresponding residues of the clade 2.1.3.2 A/Indonesia/5/05 strain (amino acid substitutions at positions Q142L, K144S, and S145P), suggesting that these amino acids are critical for binding of mAb12–1G6. Escape mutants of VN1194 selected with mAb12–1G6 carried a S145P mutation. Interestingly, mAb12–1G6 cross-neutralized clade 1 and clade 2.2.1 but not clade 2.1.3.2 or clade 2.3.4 of the H5N1 virus. We discuss the cross-reactivity, based on the amino acid sequence of the epitope.

1. Introduction

The highly pathogenic avian influenza (HPAI) H5N1 virus is a highly contagious and fatal pathogen in poultry and has been transmitted to humans with high mortality. It has raised concerns of evolving to bring about the next human influenza pandemic. Since 2003, numerous clinical cases have been reported in humans who live in close contact with infected birds in Southeast Asia [1,4]. Subsequently, a second clade of H5N1 viruses, genetically and antigenically distinct from clade 1 viruses, has been found in Indonesia and has become endemic with several subclades [3,14,15].

The influenza virus hemagglutinin (HA) is a virion surface glycoprotein and the primary target for neutralizing antibodies (Ab). HA is initially synthesized as precursor HA0 and is cleaved into HA1, variable external subunit and HA2, relatively conserved transmembranous subunit. The major part of HA1 forms the globular head domain containing the binding pocket to sialic acid expressed on host cells.

Elicitation of neutralizing Ab by vaccination is the most effective prophylaxis against influenza virus at present. Numerous studies have shown that Ab binding adjacent to the receptor-binding pocket in HA1 blocks virus attachment to the sialic receptors on host cells [7,18]. The three-dimensional structure of HA has been resolved initially for H3, and five antigenic sites (sites A, B, C, D, and E) have been mapped within the molecule [16,17]. Their corresponding antigenic sites have been mapped in the HAs of H1 and H2 subtypes [2,13]. The structure of the H5 HA molecule has recently been resolved by crystallography [6], and the sites corresponding to sites A and B of H3, have been mapped using virus escape mutants and designated as sites II and I, respectively [9] and also as sites 5 and 1, respectively in another work [10]. However, epitope mapping studies using escape mutants indicated that sites 5 and 1 were closely located in H5 HA when compared with sites A and B in H3 HA [8], and some monoclonal Abs indeed

Abbreviations: HA, hemagglutinin; HPAI, highly pathogenic avian influenza; $TCID_{50}$, 50% tissue culture infectious dose; VN1194, A/Viet Nam/1194/2004; Ind05, A/Indonesia/05/2005; Anhui01, A/Anhui/01/2005; dP, A/duck/Pennsylvania/10128/84; NC, A/NewCaledonia/20/99; scFv, single chain variable fragment.

* Corresponding author. Fax: +81 3 5791 6268.
E-mail address: morikawa@lisci.kitasato-u.ac.jp (Y. Morikawa).

0006-291X/$ - see front matter © 2011 Elsevier Inc. All rights reserved.
doi:10.1016/j.bbrc.2011.12.108

recognized with overlapping these two antigenic sites 5 and 1 [7], suggesting that the antigenic determinants in H5 HA may differ from those observed for H1 and H3 HAs.

To better understand the antigenic epitopes, especially the neutralization epitopes of H5N1 HA, we have produced a neutralizing monoclonal Ab (mAb) termed mAb12–1G6 against the pre-pandemic vaccine, NIBRG-14, for H5N1 clade 1 influenza viruses. Our epitope mapping revealed that mAb12–1G6 recognized the loop of A/Viet Nam/1194/2004 (VN1194, the parental strain of NIBRG-14) HA located near the receptor-binding domain in site 5. Our data include that mAb12–1G6 cross-neutralized the clade 2.2.1 of H5N1 virus, suggesting that mAb12–1G6 recognized the corresponding epitope of HA conserved in clade 1 and clade 2.2.1 viruses.

2. Materials and methods

2.1. Virus strains and cell culture

The following strains of influenza virus were used in this study: A/Viet Nam/1194/2004 (VN1194) (H5N1), its attenuated vaccine strain NIBRG-14, A/Indonesia/05/2005 (Ind05/PR8-RG2) (H5N1), A/turkey/Turkey/1/2005 (NIBRG-23) (H5N1), A/Anhui/01/2005 (Anhui01/PR8-RG5) (H5N1), A/duck/Pennsylvania/10128/84 (dP) (H5N2), and A/NewCaledonia/20/99 (NC) (H1N1). Madin–Darby canine kidney (MDCK) and 293T cells were maintained in Dulbecco's modified Eagle's medium containing 10% fetal bovine serum.

2.2. Virus neutralization test

A hundred 50% tissue culture infectious dose (TCID50) of influenza A H5N1 viruses was mixed with serial dilutions of mAb12–1G6 in Eagle's minimum essential medium containing 0.42% bovine serum albumin at 37 °C for 30 min. The virus-mAb mixture was inoculated to MDCK cells in a 96-well microtiter plate and the cells were incubated at 37 °C for 3–5 days. Neutralizing titers were defined as the minimum concentrations of mAb required to neutralize 100 TCID50 of H5 viruses in MDCK cells.

2.3. Selection of escape mutant

NIBRG-14 virus (10^6 $TCID_{50}$/1.2 ml) was incubated with 1 mg of mAb12–1G6 for 30 min at 37 °C. Serial dilutions of the virus-mAb mixture were inoculated to MDCK cells in a 96-well microtiter plate and the cells were incubated for 4–7 days at 37 °C. The virus culture (10^{4-5} $TCID_{50}$) was subjected to plaque purification in the presence of 2.5 μg of mAb12–1G6.

2.4. Western blot and slot blot analyses

Cells were lysed with sample buffer and subjected to SDS–PAGE followed by Western blotting. After blocking, the membrane was incubated with primary Abs and subsequently with secondary Abs conjugated with horseradish peroxidase. For slot blotting, cells were sonicated and blotted onto the membrane. The membrane was incubated with mAb12–1G6 (test Ab) and mAb25–40 (control Ab). mAb25–40 recognized a conserved region, far apart from the receptor binding pocket, in VN1194 and dP. Signal intensities by test Ab were normalized to those by control Ab. In some experiments, expression levels of HA were initially semi-quantified with control Ab using serial dilutions of cell lysates. After normalization, equivalent levels of HA proteins were blotted onto the membrane and probed with test Ab.

2.5. Expression of recombinant HA proteins

The cDNAs of the H5 HA gene were synthesized from the total virion RNAs of the NIBRG-14 and dP strains by RT-PCR. DNA construction of chimeric HAs between VN1194 and dP was carried out by PCR. Site-directed mutagenesis was carried out by using a Gene Tailor Site-Directed Mutagenesis System (Invitrogen) with the relevant primer sets. Amino acid numbering was based on the structure of H5 HA [12]. The resultant HA cDNAs were cloned into eukaryotic and *Escherichia coli* expression vectors pCDNA3 (Invitrogen) and pET14B (Novagen), respectively. Protein expression in *E. coli* was carried out by addition of isopropyl-β-D-thiogalactoside. 293T cells were transfected with the pcDNA3 vectors using Lipofectamine 2000 or LTX (Invitrogen).

2.6. Immunofluorescence assay

mAb12–1G6 was pre-labeled by using the Zenon Alexa Fluor 488 mouse IgG1 labeling kit (Invitrogen). mAb25–40 was similarly labeled with Alexa Fluor 568 as a control mAb. At 24 h post-transfection with HA expression vectors, MDCK cells were fixed with 4% paraformaldehyde and permeabilized with 0.5% Triton X-100. Following blocking, cells were incubated with the Alexa Fluor 488-labeled mAb12–1G6. After refixation, cells were incubated with the Alexa Fluor 568-labeled mAb25–40 and were observed by a microscope (BZ8000; Keyence, Osaka, Japan).

3. Results

3.1. Mapping of the epitope recognized by mAb12–1G6

We immunized mice with NIBRG-14, pre-pandemic vaccine for H5N1 clade 1 influenza virus and isolated mAb12–1G6. MAb12–1G6 reacted with HA of its parental virus, VN1194 in ELISA (Fig. S1D) and completely neutralized 100 $TCID_{50}$ of the VN1194 virus at 5 ng/50 μl. Western blotting confirmed that mAb12–1G6 reacted with VN1194 HA1 but not HA2 (data not shown).

To identify the region of VN1194 HA that is bound with mAb12–1G6, we expressed recombinant HAs with N-terminal deletions (termed del1 and del2) in *E. coli* (Fig. 1A). Western blotting revealed that mAb12–1G6 reacted with del1 (containing the globular head domain of HA1, amino acid positions 53–271) but not del2 (with a deletion of the globular head domain) (Fig. 1B), suggesting that mAb12–1G6 recognized the globular head domain of HA1. However, the *E. coli* expression system lacks post-translational modifications (e.g., glycosylation and disulfide bond formation), leading to possibly incorrect protein folding.

To assess the epitope in a more relevant expression system, we expressed full-length HA in mammalian 293T and MDCK cells. We constructed chimeric HAs between VN1194 (H5N1) and dP (H5N2), the latter of which did not react with mAb12–1G6 (Fig. 1C). mAb12–1G6 reacted with chimeras A and C containing the globular head domain derived from VN1194 HA but not with chimeras B and D containing that of dP HA (Fig. 1C). mAb12–1G6 still failed to bind chimeric HA containing a smaller region of dP HA (amino acid positions 116–256) (chimera E) but recovered when the region was limited to amino acid positions 183–227 (chimera G) (Fig. 1C). These findings were confirmed when the signal intensity obtained with mAb12–1G6 was normalized by that obtained with mAb25–40. These data suggest that mAb12–1G6 recognized the amino acid positions 116–183, a region partly composed of the receptor-binding pocket in HA1.

To determine the epitope for mAb12–1G6, we carried out alanine scanning mutagenesis at the surface residues within amino acid positions 128–228 (see Fig. 3D). Western blotting with 293T

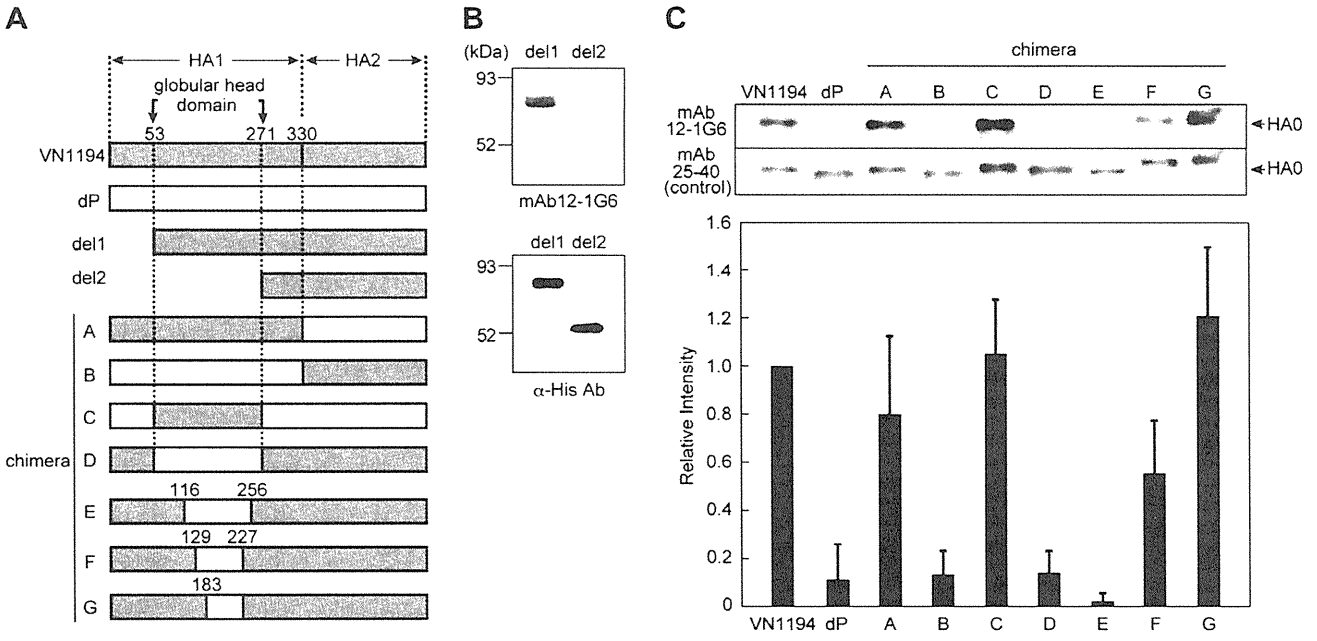

Fig. 1. Reactivities of mAb12–1G6 with truncated and chimeric VN1194 HAs. (A) Schematic representation of truncated/chimeric HAs of influenza VN1194 (H5N1) viruses. Amino acid numbering is based on the H5 HA. The globular head domain of HA1 corresponds to a 53–271 region. The position 330 indicates the HA1/HA2 cleavage site. VN1194 HA is colored in gray and dP (H5N2) HA is in white. (B) Reactivities of mAb12–1G6 with truncated VN1194 HAs. The HAs (del1 and del2) with 6 histidine tags were expressed in *E. coli* and subjected to Western blotting using mAb12–1G6 and anti-histidine-tag Ab. (C) Reactivities of mAb12–1G6 with chimeric HAs between VN1194 and dP. 293T cells expressing chimeric HAs were sonicated and subjected to Western blotting using mAbs12–1G6 and 25–40. Intensities of signals were measured using ImageJ software and relative intensities (mAb12–1G6 to mAb25–40) were calculated. Data were shown as means with standard deviations from three independent experiments.

cell lysates showed that mAb12–1G6 did not react with the VN1194 HA mutants only when they contained single Y141A, Q142A, G143A, K144A, and K193A substitutions (Fig. 2A). Since Western blotting is inappropriate for the analysis of conformational epitopes, cell lysates without protein denaturation were subjected to slot blotting. In this assay, mAb12–1G6 similarly failed to react with the Q142A, G143A, or K144A mutants (Fig. 2B). The use of mAb25–40 (as a control) showed that comparable levels of HAs were applied in both assays. Consistent with the data by these assays, when the HA mutants were expressed in MDCK cells and were subjected to indirect immunofluorescence analysis, mAb12–1G6 did not detect the Q142A, G143A, or K144A mutants (Fig. 2C). Thus, our surface scanning mutagenesis defined the amino acids 142, 143, and 144 of VN1194 HA as determinants for the mAb12–1G6 binding. In the H5 HA1 structure analyzed by crystallography [5,12], the region we mapped was located near the receptor-binding pocket (Fig. 3C), suggesting that mAb12–1G6 may conformationally inhibit HA binding to sialic acid receptor.

To determine accurately the epitope for mAb12–1G6, 3 escape mutants of the VN1194 virus were selected in the presence of mAb12–1G6. Sequencing of the entire HA1 region revealed that all escape mutants carried only S145P substitution.

3.2. Neutralizing activity of mAb12–1G6 against clade 2 viruses and reactivity of mAb12–1G6 with clade 1 H5 HA (VN1194) derivatives containing the corresponding epitope of clade 2.1.3.2 H5 HA (Ind05)

To test whether the mAb12–1G6 generated against the clade 1 VN1194 virus also neutralized various clade 2 H5N1 viruses, VN1194 (clade 1), Ind05/PR8-RG2 (clade 2.1.3.2), NIBRG-23 (clade 2.2.1), and Anhui01/PR8-RG5 (clade 2.3.4) were used. mAb12–1G6 did not neutralize clade 2.1.3.2 or 2.3.4 viruses even at 10 μg/50 μl but did cross-neutralize clade 2.2.1 virus at 5 ng/50 μl, a concentration which was comparable with the concentration to neutralize clade 1 VN1194 virus.

To investigate whether the neutralization failure of mAb12–1G6 against the clade 2.1.3.2 Ind05 virus was due to amino acid variations at the corresponding epitope, the amino acids at positions 142, 144, and 145 of VN1194 HA were replaced with the corresponding residues of the clade 2.1.3.2 Ind05 HA (Q142L, K144S, and S145P, respectively) (Fig. 3A). Slot blotting analysis revealed that mAb12–1G6 did not recognize the H5 HA with S145P substitution. Single Q142L and K144S substantially reduced but did not abolish the reactivity with mAb12–1G6. A combination of these substitutions abolished the reactivity with mAb12–1G6 (Fig. 3B). Collectively, our data indicate that the S145P substitution is crucial for the mAb12–1G6 reactivity, whereas K144R substitution (e.g., clade 2.2.1 NIBRG-23) is well tolerated. A careful observation of the amino acid sequences of the corresponding epitope among the clade 2 viruses indicated that glutamine at position 142 and serine at position 145 were conserved in clade 1 and 2.2.1 viruses and at least, the latter was mutated to proline in the clade 2.1.3.2 and 2.3.4 viruses (Fig. 3A).

3.3. Reactivity of scFv12–1G6 with H5 and H1 HAs

To further confirm the epitope recognized by mAb12–1G6, we expressed and purified single-chain variable fragment (scFv) of mAb12–1G6 in which the genes of the variable heavy and light chains were joined with a polypeptide linker. When the reactivity of scFv12–1G6 was tested by sandwich-ELISA using H5 HAs expressed in 293T cells, scFv12–1G6 showed higher binding affinity to clade 1 VN1194 and clade 2.2.1 NIBRG-23 HAs than dP HA and almost lost the affinity to the VN1194 HA derivative containing Q142L, K144S, and S145P substitutions (Fig. S1A). These binding profiles were similar to those of our original mAb12–1G6. Slot blotting showed that mAb12–1G6 cross-reacted with both VN1194 and NC (H1) viruses (Fig. S1B), possibly through the binding avidity

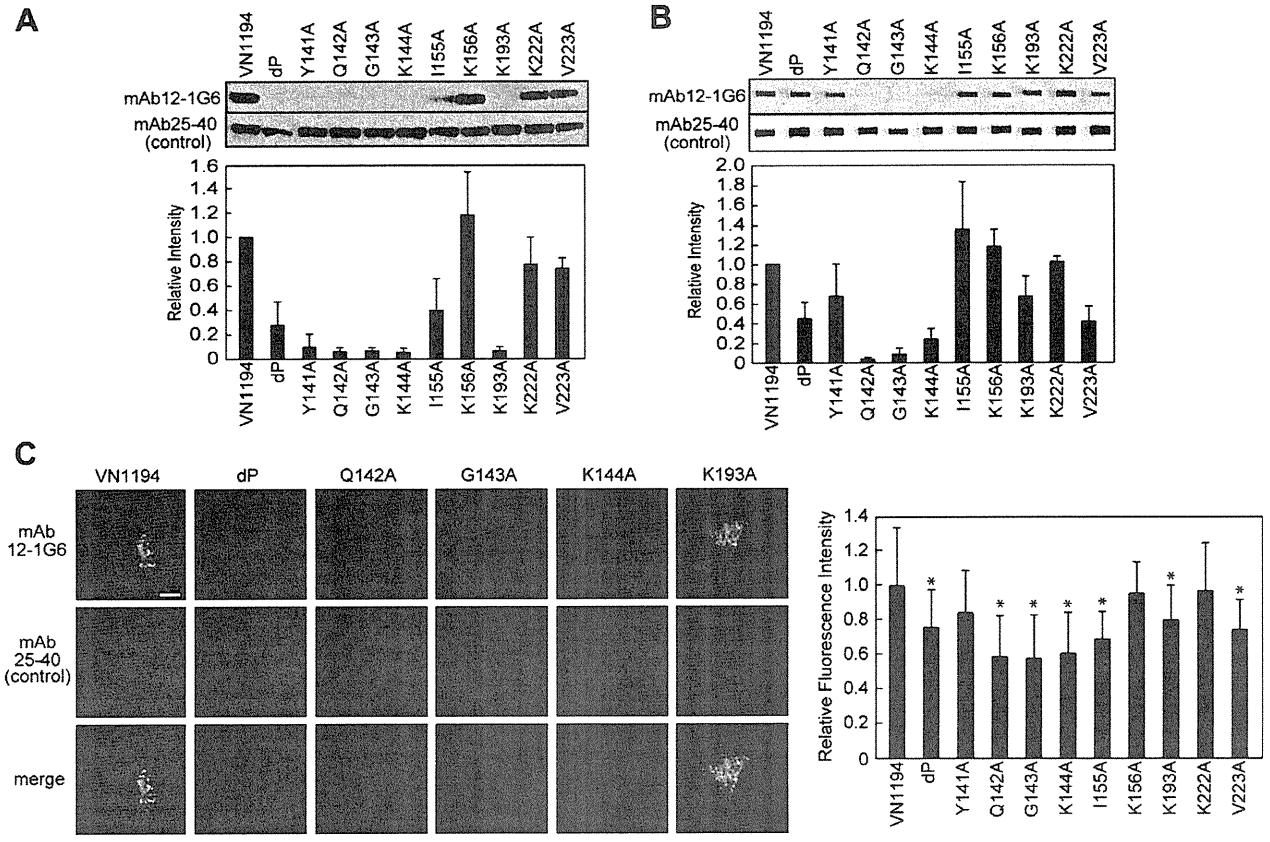

Fig. 2. Reactivities of mAb12–1G6 with VN1194 HA mutants containing amino acid substitutions. 293T cells expressing HA constructs containing amino acid substitutions (indicated) were sonicated and subjected to Western blotting (A) and slot blotting (B) using mAb12–1G6 and mAb25–40 (as a control). In each assay, signal intensities were measured using ImageJ software and relative intensities (mAb12–1G6–mAb25–40) were calculated. (C) MDCK cells expressing HA constructs with amino acid substitutions (indicated) were subjected to indirect immunofluorescence assay using mAb12–1G6 (green) and mAb25–40 (as a control) (red). Nuclei were stained with DAPI (blue). Fluorescence intensities were measured using ImageJ software with the "RGB Measure" plug-in and relative fluorescence intensities (mAb12–1G6–mAb25–40) were calculated. All micrographs were shown at the same magnification. Bar, 10 μm. All graph data were indicated as means with standard deviations from three independent experiments. *, $p < 0.01$.

of mAb12–1G6. To test this possibility, the VN1194 and NC viruses were slot-blotted to the membrane and probe with scFv12–1G6, indicating that scFv did not bind to the NC virus but only detected the VN1194 virus (Fig. S1C). When the binding affinities of mAb12–1G6 and scFv12–1G6 were compared by sandwich-ELISA, the results indicated that scFv12–1G6 showed an approximately 1000-fold lower binding affinity, although both mAb12–1G6 and scFv12–1G6 bound to VN1194 HA and NIBRG-23 HA in a dose-dependent manner (Fig. S1D and E). Much lower affinity of scFv than affinity of mAb has been reported elsewhere [11]. ScFv12–1G6 failed to bind to VN1194 HA derivative containing Q142L, K144S, and S145P substitutions, confirming that mAb12–1G6 and scFv12–1G6 specifically recognized the epitope composed of an exposed loop near the receptor-binding site [12].

4. Discussion

In this study, we obtained mAb12–1G6, which neutralized the clade 1 (VN1194) and clade 2.2.1 (NIBRG-23) but not clade 2.1.3.2 (Ind05) or clade 2.3.4 (Anhui01) H5N1 influenza viruses. Epitope mapping on VN1194 HA revealed that mAb12–1G6 recognized the exposed loop (amino acid positions 140–145 of HA1) corresponding to antigenic site A in H3 HA (Fig. 3C).

Phylogenetic analysis of H5 HA genes from 2004 and 2005 has shown two distinct lineages, termed clade 1 and 2 [3]. Comparison of their amino acid sequences and analysis of crystal structures have identified 13 antigenic variations, many of which are mainly clustered around the receptor binding domain [12]. Indeed, the epitope in clade 1 VN1194 HA recognized by mAb12–1G6 exhibited substitutions Q142L, K144S, and S145P in clade 2.1.3.2 Ind05 HA (Fig. 3A). A comparison of the amino acid sequence in the globular head domain between the VN1194 and Ind05 HAs revealed 12 amino acid differences (Fig. 3D). In the three-dimensional structure of the globular domain, the 6 amino acids (at positions 133, 142, 143, 144, 145, and 193) out of the 12 amino acids were located near the epitope and/or the receptor-binding pocket (Fig. 3C, left). Site-directed substitutions L133S (data not shown) and K193A (Fig. 2B and C) showed no reduction in the reactivity by mAb12–1G6, suggesting that the amino acid differences in the proximity of the epitope were not involved in the reactivity by mAb12–1G6.

A careful sequence comparison around the epitope (Fig. 3A) showed that clade 2.1.3.2 Ind05 and clade 2.3.4 Anhui01, neither of which was neutralized by mAb12–1G6, had common amino acid propensities (polarity or hydrophobicity) in the epitope. For example, lysine (hydrophilic, basic) at position 144 in clade 1 VN1194 HA was substituted for serine in clade 2.1.3.2 Ind05 and for threonine in clade 2.3.4 Anhui01, both of which were hydrophilic and polar. However, when the glutamine at position 142 and the lysine at 144 were singly substituted by leucine and serine within the clade 1 HA, respectively, the reactivity with mAb12–1G6 was reduced but not abolished (Fig. 3B), suggesting that these substitutions, unless combined, may be tolerated. The K144R substitution showed no reduction in mAb12–1G6 binding (Fig. 3B) and in fact, mAb12–1G6 neutralized the clade 2.2.1 (NIBRG-23) strain, which contains a K144R substitution in the epitope.

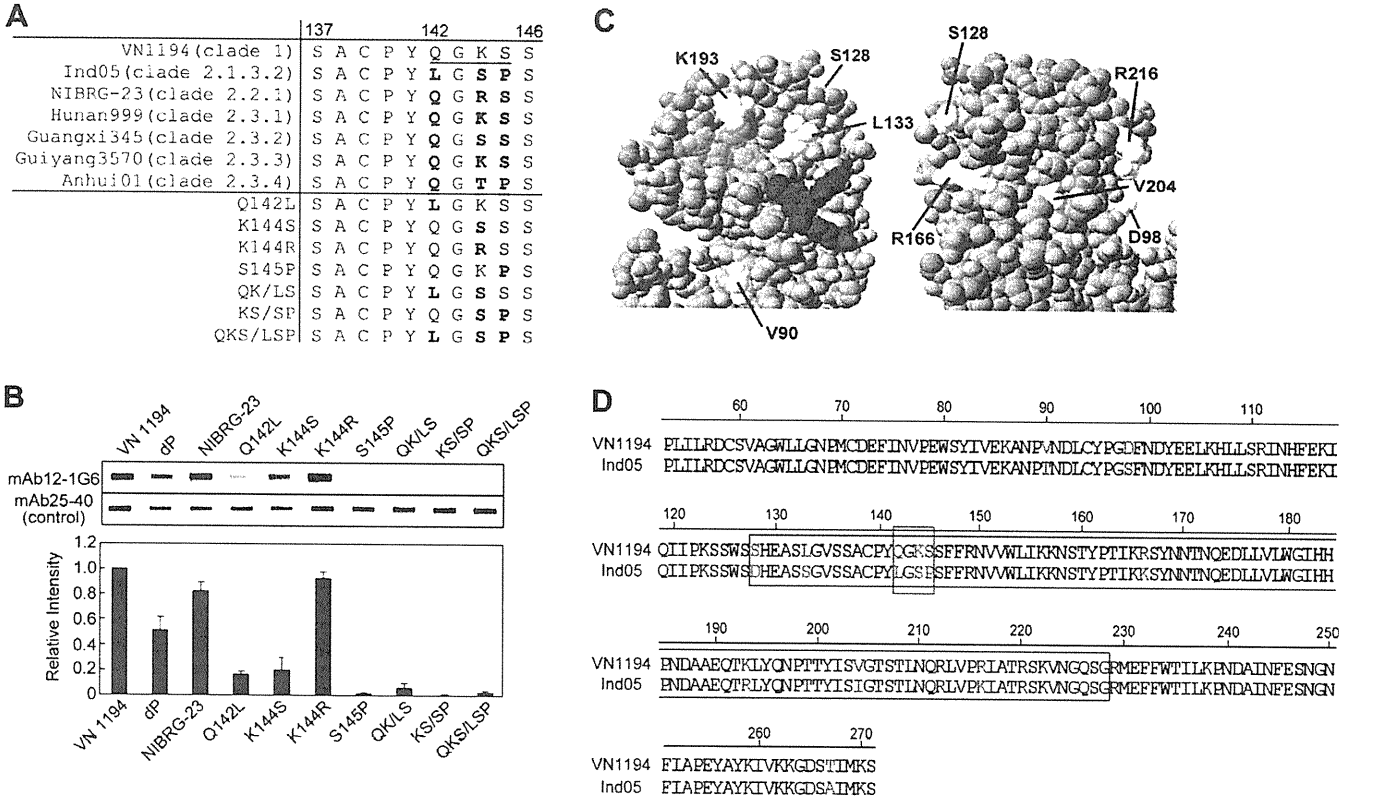

Fig. 3. Defining of the amino acids recognized by mAb12–1G6. (A) Amino acid sequences in and around the epitope recognized by mAb12–1G6 in VN1194 (clade 1), Ind05 (clade 2.1.3.2), NIBRG-23 (clade 2.2.1), A/chicken/Hunan/999/2005 (Hunan999) (clade 2.3.1), A/Goose/Guangxi/345/2005 (Guangxi345) (clade 2.3.2), A/chicken/Guiyang/3570/2005 (Guiyang3570) (clade 2.3.3), and Anhui01 (clade 2.3.4) HAs, and VN1194 HA derivatives containing the corresponding amino acid substitutions. Amino acid diversity is observed at positions 142 (yellow), 144 (blue), and 145 (orange). The epitope recognized by mAb12–1G6 was underlined and mutated amino acids were indicated by bold. (B) The reactivity of mAb12–1G6 with VN1194 HA derivatives containing amino acid substitutions to clade 2 (at positions 142, 144, and 145). 293T cells expressing the HAs containing the single, double, and triple amino acid substitutions were subjected to slot blotting as described in the legend for Fig. 2B. Signal intensities were measured using ImageJ software and relative intensities (means with standard deviations) were calculated form three independent experiments. (C) The epitope recognized by mAb12–1G6 and the location of amino acid differences between VN1194 and Ind05 HAs on the globular head domain. The image of the head domain in H5 HA was generated from the Protein Data Bank (PDB accession number 2IBX) and with Swiss-Pdb Viewer. The epitope recognized by mAb12–1G6 (red), the mutated amino acids between VN1194 and Ind05 HAs (yellow), and the receptor-binding pocket (blue) were highlighted. (D) The amino acid sequences of the globular head domain of the VN1194 and Ind05 HAs. The residues boxed in yellow indicate different amino acids between VN1194 and Ind05. The epitope recognized by mAb12–1G6 was boxed by red line. The region boxed by black line includes the surface amino acids examined by alanine scanning mutagenesis in this study.

More importantly, the serine at position 145 in clade 1 was replaced by proline in clade 2.1.3.2 and clade 2.3.4. The S145P substitution, when introduced into VN1194 HA, completely abolished the reactivity by mAb12–1G6 (Fig. 3B). This finding was further highlighted when the escape mutants of VN1194 were selected in the presence of mAb12–1G6. Consistent with our data, some neutralizing mAbs described previously failed to react with escape mutants from clade 1 A/Viet Nam/1203/04 (H5N1) virus, only when the viruses contained amino acid substitutions at position 145 [7]. Altogether, the data suggest that the proline at position 145 is significantly involved in the loop structure in antigenic site A. Our escape mutants only contained the S145P substitution, suggesting that mAb12–1G6 may specifically recognize the loop structure. Alternatively, it is possible that the substitution at position 145 has initially been selected in the presence of mAb12–1G6. A comparison of the amino acids at position 145 in H5N1 HA sequences showed proline in clade 2.1.3.2 (Ind05) and clade 2.3.4 (Anhui01) but serine in clades 2.3.1, 2.3.2, and 2.3.3. Since the serine at position 145 is conserved in clade 2.3.1–2.3.3 viruses, it is possible, although is not proven, that mAb12–1G6 may have cross-clade neutralizing activity against these clade viruses.

Acknowledgments

We thank Dr. J.M. Wood (National Institute for Biological Standards and Control, UK) for providing attenuated H5N1 vaccine strain, NIBRG-14 and Dr. H. Kida (Hokkaido University, Japan) for the total virion RNAs of the dP strains. This work was supported by a grant from the Ministry of Health, Labor, and Welfare of Japan, by a Grant-in-Aid for Scientific Research from the Japan Society for the Promotion of Science.

Appendix A. Supplementary data

Supplementary data associated with this article can be found, in the online version, at doi:10.1016/j.bbrc.2011.12.108.

References

[1] D. Areechokchai, C. Jiraphongsa, Y. Laosiritaworn, W. Hanshaoworakul, M. O'Reilly, Centers for Disease Control and Prevention (CDC), Investigation of avian influenza (H5N1) outbreak in humans–Thailand, 2004, MMWR Morb. Mortal. Wkly. Rep. 55 Suppl 1 (2006) 3–6.

[2] A.J. Caton, G.G. Brownlee, J.W. Yewdell, W. Gerhard, The antigenic structure of the influenza virus A/PR/8/34 hemagglutinin (H1 subtype), Cell 31 (1982) 417–427.

[3] H. Chen, G.J. Smith, K.S. Li, J. Wang, X.H. Fan, J.M. Rayner, D. Vijaykrishna, J.X. Zhang, L.J. Zhang, C.T. Guo, C.L. Cheung, K.M. Xu, L. Duan, K. Huang, K. Qin, Y.H. Leung, W.L. Wu, H.R. Lu, Y. Chen, N.S. Xia, T.S. Naipospos, K.Y. Yuen, S.S. Hassan, S. Bahri, T.D. Nguyen, R.G. Webster, J.S. Peiris, Y. Guan, Establishment of multiple sublineages of H5N1 influenza virus in Asia: implications for pandemic control, P. Natl. Acad. Sci. USA 103 (2006) 2845–2850.

[4] P.N. Dinh, H.T. Long, N.T. Tien, N.T. Hien, T.Q. Mai le, H. Phong le, V. Tuan le, H. Van Tan, N.B. Nguyen, P. Van Tu, N.T. Phuong, World Health Organization/Global Outbreak Alert and Response Network Avian Influenza Investigation

Team in Vietnam, Risk factors for human infection with avian influenza A H5N1, Vietnam, 2004, Emerg. Infect. Dis. 12 (2006) 1841–1847.
[5] Y. Ha, D.J. Stevens, J.J. Skehel, D.C. Wiley, H5 avian and H9 swine influenza virus hemagglutinin structures: possible origin of influenza subtypes, EMBO J. 21 (2002) 865–875.
[6] Y. Ha, D.J. Stevens, J.J. Skehel, D.C. Wiley, X-ray structures of H5 avian and H9 swine influenza virus hemagglutinins bound to avian and human receptor analogs, P. Natl. Acad. Sci. USA 98 (2001) 11181–11186.
[7] N.V. Kaverin, I.A. Rudneva, E.A. Govorkova, T.A. Timofeeva, A.A. Shilov, K.S. Kochergin-Nikitsky, P.S. Krylov, R.G. Webster, Epitope mapping of the hemagglutinin molecule of a highly pathogenic H5N1 influenza virus by using monoclonal antibodies, J. Virol. 81 (2007) 12911–12917.
[8] N.V. Kaverin, I.A. Rudneva, N.A. Ilyushina, A.S. Lipatov, S. Krauss, R.G. Webster, Structural differences among hemagglutinins of influenza A virus subtypes are reflected in their antigenic architecture: analysis of H9 escape mutants, J. Virol. 78 (2004) 240–249.
[9] N.V. Kaverin, I.A. Rudneva, N.A. Ilyushina, N.L. Varich, A.S. Lipatov, Y.A. Smirnov, E.A. Govorkova, A.K. Gitelman, D.K. Lvov, R.G. Webster, Structure of antigenic sites on the hemagglutinin molecule of H5 avian influenza virus and phenotypic variation of escape mutants, J. Gen. Virol. 83 (2002) 2497–2505.
[10] M. Philpott, C. Hioe, M. Sheerar, V.S. Hinshaw, Hemagglutinin mutations related to attenuation and altered cell tropism of a virulent avian influenza A virus, J. Virol. 64 (1990) 2941–2947.
[11] Y. Reiter, U. Brinkmann, B. Lee, I. Pastan, Engineering antibody Fv fragments for cancer detection and therapy: disulfide-stabilized Fv fragments, Nat. Biotechnol. 14 (1996) 1239–1245.
[12] J. Stevens, O. Blixt, T.M. Tumpey, J.K. Taubenberger, J.C. Paulson, I.A. Wilson, Structure and receptor specificity of the hemagglutinin from an H5N1 influenza virus, Science 312 (2006) 404–410.
[13] E. Tsuchiya, K. Sugawara, S. Hongo, Y. Matsuzaki, Y. Muraki, Z.N. Li, K. Nakamura, Antigenic structure of the hemagglutinin of human influenza A/H2N2 virus, J. Gen. Virol. 82 (2001) 2475–2484.
[14] R.G. Webster, E.A. Govorkova, H5N1 influenza–continuing evolution and spread, N. Engl. J. Med. 355 (2006) 2174–2177.
[15] WHO/OIE/FAO H5N1 Evolution Working Group, Continued evolution of highly pathogenic avian influenza A (H5N1): updated nomenclature, Influenza and Other Respiratory Viruses 6 (2011) 1-5.
[16] D.C. Wiley, I.A. Wilson, J.J. Skehel, Structural identification of the antibody-binding sites of Hong Kong influenza hemagglutinin and their involvement in antigenic variation, Nature 289 (1981) 373–378.
[17] I.A. Wilson, J.J. Skehel, D.C. Wiley, Structure of the hemagglutinin membrane glycoprotein of influenza virus at 3 A resolution, Nature 289 (1981) 366–373.
[18] R. Yoshida, M. Igarashi, H. Ozaki, N. Kishida, D. Tomabechi, H. Kida, K. Ito, A. Takada, Cross-protective potential of a novel monoclonal antibody directed against antigenic site B of the hemagglutinin of influenza A viruses, PLoS Pathog. 5 (2009) e1000350.

Biologicals 40 (2012) 96–99

Contents lists available at SciVerse ScienceDirect

Biologicals

journal homepage: www.elsevier.com/locate/biologicals

Application of deglycosylation to SDS PAGE analysis improves calibration of influenza antigen standards

Ruth Harvey [a], Michelle Hamill [b], James S. Robertson [a], Philip D. Minor [a], Galina M. Vodeiko [c], Jerry P. Weir [c], Hitoshi Takahashi [d], Yuichi Harada [d], Shigeyuki Itamura [d], Pearl Bamford [e], Tania Dalla Pozza [e], Othmar G. Engelhardt [a,*]

[a] Division of Virology, National Institute for Biological Standards and Control, Health Protection Agency, Blanche Lane, South Mimms, Potters Bar, Hertfordshire EN6 3QG, United Kingdom
[b] BioStatistics, National Institute for Biological Standards and Control, Health Protection Agency, Blanche Lane, Potters Bar, Hertfordshire EN6 3QG, United Kingdom
[c] Division of Viral Products, Center for Biologics Evaluation and Research (CBER), Food and Drug Administration (FDA), Bethesda, MD 20892, USA
[d] Center for Influenza Virus Research, National Institute of Infectious Diseases, Gakuen 4-7-1, Musashimurayama-shi, Tokyo 208 0011, Japan
[e] Therapeutic Goods Administration, PO Box 100, Woden ACT 2606, Australia

ARTICLE INFO

Article history:
Received 23 September 2011
Received in revised form
21 November 2011
Accepted 20 December 2011

Keywords:
Influenza
Vaccine
Standardisation
HA
Standards
Deglycosylation
Calibration

ABSTRACT

Each year the production of seasonal influenza vaccines requires antigen standards to be available for the potency assessment of vaccine batches. These are calibrated and assigned a value for haemagglutinin (HA) content. The calibration of an antigen standard is carried out in a collaborative study amongst a small number of national regulatory laboratories which are designated by WHO as Essential Regulatory Laboratories (ERLs) for the purposes of influenza vaccine standardisation. The calibration involves two steps; first the determination of HA protein in a primary liquid standard by measurement of total protein in a purified influenza virus preparation followed by determination of the proportion of HA as determined by PAGE analysis of the sample; and second, the calibration of the freeze-dried reference antigen against the primary standard by single radial immunodiffusion (SRD) assay. Here we describe a collaborative study to assess the effect of adding a deglycosylation step prior to the SDS-PAGE analysis for the assessment of relative HA content. We found that while the final agreed HA value of the samples tested was not significantly different with or without deglycosylation, the deglycosylation step greatly improved between-laboratory agreement.

1. Introduction

Vaccination against seasonal and pandemic influenza virus remains an important strategy to reduce morbidity and mortality associated with the disease [1]. Inactivated seasonal trivalent vaccines produced by numerous manufacturers worldwide currently contain standardized amounts of the haemagglutinin (HA) from an A/H1N1, A/H3N2 and B strain of influenza virus. Due to rapid mutation in influenza viruses (antigenic drift), the World Health Organisation (WHO) makes biannual recommendations for the strains to be used in the formulation of influenza vaccine, based on worldwide surveillance and characterisation of circulating strains [2]; as a result, one or more strains in the vaccine typically needs to be updated (reviewed in [3] and [4]). The potency of each lot of vaccine produced is determined by the single radial immunodiffusion assay (SRD) which has been the WHO recommended assay for influenza vaccine potency determination since 1979 [5,6]. The use of SRD for quantitation of HA antigen in vaccine requires a set of two reference reagents, an HA antigen standard and an anti-HA sheep antiserum, that match the vaccine strain. Thus, new reagents must be prepared each time there is a change in the WHO recommended vaccine strain.

The anti-HA sheep antiserum is raised against purified HA from the recommended strain. The HA antigen reagent is typically a preparation of inactivated whole virus donated by a vaccine manufacturer that is freeze-dried by, or on behalf of, an Essential Regulatory Laboratory (ERL). To calibrate this reagent, a primary liquid standard (PLS) is prepared by an ERL from a purified virus preparation of the recommended strain. The total protein within a PLS is determined using a standard protein quantitative assay (e.g. Lowry) whilst the proportion of HA protein within the PLS is determined from a densitometric analysis of the viral proteins separated by SDS-PAGE run under both reduced and non-reduced conditions [7]. In this assay it is the protein bands of the reduced samples that are used in the quantitation, with the non-reduced

* Corresponding author. Tel.: +44 01707 641000; fax: +44 01707 641366.
E-mail address: othmar.engelhardt@nibsc.hpa.org.uk (O.G. Engelhardt).

1045-1056/$36.00
doi:10.1016/j.biologicals.2011.12.009

samples run alongside to aid in identification of the protein bands where a degree of co-migration occurs. Densitometric analysis of protein bands in the non-reduced samples is not optimal for accurate quantitation because a lot of the proteins co-migrate or are present as higher molecular weight aggregates.

The calibration of a PLS is performed in a collaborative study within WHO designated ERLs, namely the Centre for Biologics Evaluation and Research (CBER), Food and Drug Administration, USA, the National Institute for Biological Standards and Control (NIBSC), Health Protection Agency, UK, the National Institute of Infectious Diseases (NIID), Japan and the Therapeutic Goods Administration (TGA), Australia. The data from all laboratories are collated so that an HA content value in μg can be assigned to the PLS. The primary standard is then used in SRD to calibrate the freeze-dried secondary standard, which is the antigen reference material used by manufacturers as well as National Control Laboratories for the potency testing of an influenza vaccine.

Quantitation of peaks from the densitometric analysis of the SDS-PAGE of purified virus preparations is sometimes technically challenging due to various degrees of co-migration of the relevant protein bands. This phenomenon is strain-dependent and not predictable. Recently we described a modification of the SDS-PAGE method to include deglycosylation of samples before analysis [8]. Because deglycosylation shifts the mobility of the HA bands within the SDS-PAGE gels, this modification improved the reproducibility of the quantitation of the HA in our laboratory. Therefore, a collaborative study was set up among the ERLs to assess the modified method in comparison to standard in-house methods of the ERLs for the calibration of HA antigen reagent.

2. Materials and methods

2.1. Study design

A panel of purified preparations of four viruses was sent to each of the four ERLs. Each laboratory tested the samples for HA content (% HA) using their standard in-house methodology and then tested the samples following a prescribed method for the deglycosylation method. Data was returned to NIBSC, collated and statistical analysis carried out to assess the reproducibility of the alternative methods within and between laboratories. Each sample was tested by each laboratory by each method at least three times, so all data shown are the average of at least 3 individual data points.

2.2. Virus concentrates

A panel of viruses was made comprised of PR8 (H1N1), NYMC X-157 (H3N2), NYMC X-161b (H3N2) and IVR-116 (H1N1). All viruses were grown in 11 day old embryonated hens' eggs. Allantoic fluid was harvested 72 h post infection and was clarified at high speed (10 000 rpm, 30 min, 4 °C, in a Beckman SW28 rotor). Virus was pelleted by centrifugation (25 000 rpm, 90 min at 4 °C in a Beckman SW28 rotor). Virus pellets were resuspended in 1 ml PBS and loaded onto an 11 ml, 10–40% continuous sucrose gradient which was centrifuged at 35 000 rpm for 35 min at 4 °C in a Beckman SW41 rotor. The virus band was harvested, made up to an appropriate volume in PBS, pelleted by centrifugation (25 000 rpm, 90 min, 4 °C, in Beckman SW28 rotor) and the final virus pellet resuspended in PBS (10 μl per egg used).

2.3. SDS-PAGE analysis

SDS-PAGE analysis was performed in each laboratory according to standard protocols. For the gel in Fig. 1 the following method was used. One to 3 μL of virus concentrate (approximately 10 μg total protein) was mixed with water to a total volume of 10 μl. Loading dye (2.5 μl) with 2% (v/v) β-mercaptoethanol as reducing agent was added to each sample. Samples were heated to 95 °C for 3 min prior to loading onto the gels. Ten percent Bis-Tris gels were used and run at 125 V for 90 min using MOPS buffer (Invitrogen) followed by staining using Colloidal Blue stain (Invitrogen). Quantitation was carried out using an Imagescanner and associated software (GE healthcare). The content of HA for each sample was calculated as follows; firstly, the total viral protein value, in arbitrary units, was calculated by summing the quantitated values for the HA1, HA2, NP and M1 bands on the gel (these were the predominant bands observed in the SDS-PAGE gels of purified virus). The HA1 and HA2 values were summed to give the total HA value. The percent HA of total protein was calculated by dividing the total HA by the total protein multiplied by 100.

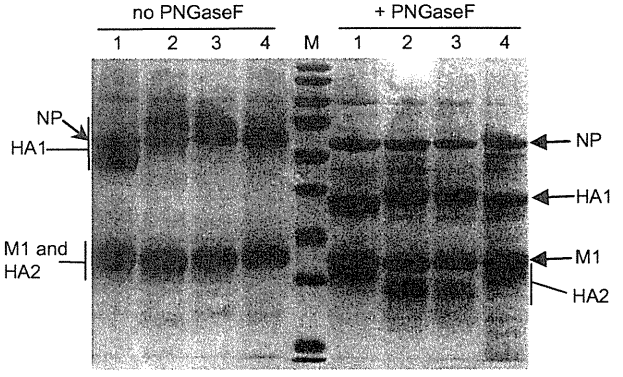

Fig. 1. SDS PAGE analysis of viruses. The four viruses included in the panel to be tested by each laboratory were analysed by SDS PAGE. Sample 1, PR8; 2, NYMC X-157; 3, NYMC X-161b; 4, IVR-116. All virus samples were reduced. Viruses were compared either deglycosylated (PNGase F +), or non deglycosylated (PNGase F -).

2.4. Deglycosylation using PNGase F

Deglycosylation was achieved using PNGase F (New England Biolabs). Approximately 10 μg (typically 1–3 μl) of each virus concentrate was denatured according to the PNGase F manufacturer's instructions in a total reaction volume of 10 μl and samples were incubated at 37 °C overnight (approx. 16 h) with 1 μl of a 1/20 dilution of PNGase F enzyme in buffer provided by the manufacturer and 1% final concentration NP40 (provided with enzyme). Loading dye (2.5 μl) with 2% (v/v) β-mercaptoethanol as reducing agent was added to each sample. Samples were heated to 95 °C for 3 min prior to loading onto SDS-PAGE gels. Gels were run and stained as above.

2.5. Statistical analysis

Statistical analysis was performed using Minitab 15 statistical software. The analysis was performed using a general linear model with the Tukey method for pair-wise comparisons [9].

3. Results

A panel of seasonal viruses was assembled and assessed by SDS PAGE analysis with and without deglycosylation (Fig. 1). The results show that when the virus samples are run under reducing conditions with no PNGaseF treatment, there are varying degrees of co-migration between the viral protein bands. Of note, the NA protein often cannot be seen on gels, as there is not enough present to produce a visible band and, as a glycoprotein, it is diffuse without deglycosylation. When deglycosylation is used, a discrete NA band may be apparent for some viruses, but, as observed in this study,

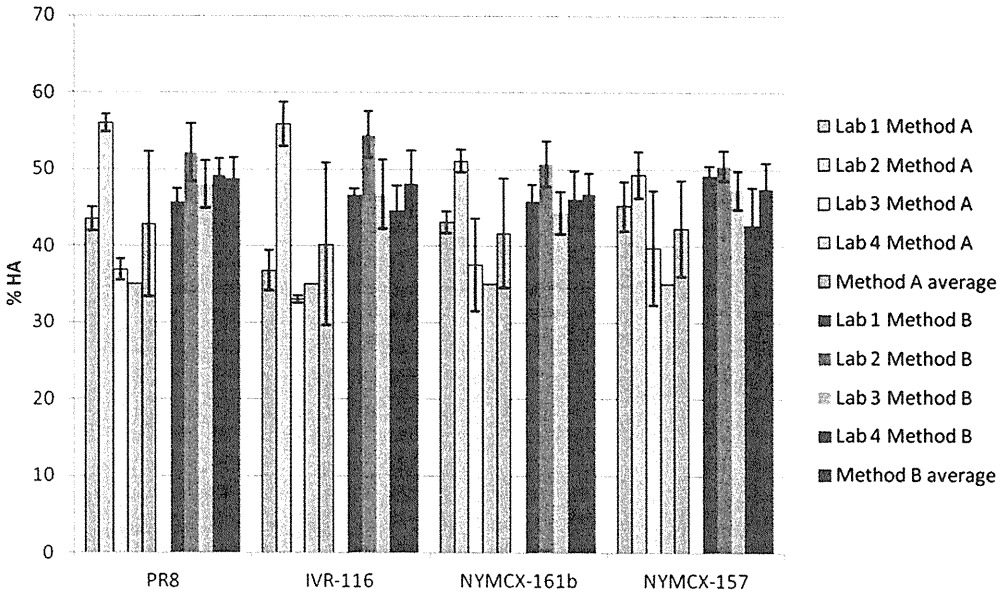

Fig. 2. HA content of viruses. Each of the four laboratories measured HA content using their in-house method (Method A) or the prescribed deglycosylation protocol (Method B). Results shown are the average of ≥3 separate experiments for each method and each sample, except for lab 4 Method A as explained in the text. The overall average for each virus/method is also shown (average). Error bars denote standard deviations.

this is not always the case. Running the same set of virus samples under reducing conditions after deglycosylation leads to much better separation of the viral proteins, which allows more accurate and reproducible quantitation.

We analysed %HA values with (method B) or without (method A) deglycosylation treatment of samples, based on the original in-house SDS-PAGE procedures of each laboratory. In order to compare the reproducibility of the methods among laboratories a single method for calculating the %HA content as described in materials and methods was used. One participant, laboratory 4, did not have an in-house experimental method for the quantitation of %HA and uses an assumed value of 35% instead, based on historical experience for assignment of HA content to the PLS. Therefore, no method A was included in the statistical analysis for laboratory 4, but an assumed value 35% is included in the results of the study shown in Fig. 2.

Tables 1 (method A) and 2 (method B) show individual means for each method, lab and virus calculated using data from replicate responses, expressed as %HA protein of the total viral protein in a sample. Overall means for each lab were calculated as the mean of the four individual virus means within the lab, and overall means for each virus were calculated as the mean of the individual lab means for each of the viruses.

The results for all viruses were similar for both methods, with an overall mean of 44%HA for method A and a mean of 48%HA for method B.

Within a virus, variability between labs depended on the method, with method B appearing to have better agreement between labs than method A. This is reflected by the between lab CV for individual viruses, which ranged from 10% to 30% for method A and 5%–9% for method B. Similarly, the overall between lab variability was lower for method B than for method A (6% and 19% respectively), indicating an overall improved agreement between labs for method B as compared to method A.

Between replicate variability (Tables 3 and 4) was assessed by pooling individual CVs calculated from replicate responses within each lab and virus. Estimates were pooled both across viruses within a lab to give a pooled estimate of within lab, between replicate variation, and across labs within a virus to give a pooled estimate of within virus, between replicate variation. An overall pooled estimate of between replicate variability for each method was calculated using the average of the pooled standard deviations and the overall mean for the particular method.

Overall pooled estimates for both methods were similar (7.0% for method A and 5.8% for method B) indicating similar between replicate variability for the two methods.

For method A, pooled CVs within a lab and virus were less than 10%, with the exception of lab 3 which was marginally more variable at 13.6%. This was due to two viruses, NYMC X-161b and NYMC X-157 which had higher between replicate variability (16.1% and 18.6% respectively) than viruses PR8 and IVR-116 (3.9% and 1.3% respectively). This is reflected also by the pooled within virus CVs which are higher for NYMC X-161b and NYMC X-157 (9.1% and 9.4%) than for PR8 and IVR-116 (3.5% and 5.9%). Comparing the pooled within lab CVs and the between virus CVs (Tables 1 and 3) and taking into

Table 1
Method A lab and virus means with between-lab %CVs.

Virus	Method A			Virus mean	Between lab %CV
	Lab 1	Lab 2	Lab 3		
IVR-116	36.85	55.88	33.02	**41.92**	**29.21**
NYMC X-157	45.21	49.32	39.76	**44.76**	**10.71**
NYMC X-161b	43.10	51.07	37.56	**43.91**	**15.47**
PR8	43.57	56.00	36.96	**45.51**	**21.24**
Lab Mean	**42.18**	**53.07**	**36.83**	**44.03 (overall)**	**18.80**

Values shown are the averages of at least 3 independent experiments.
Bold indicates means between viruses and/or labs, as well as CVs.

Table 2
Method B lab and virus means with between-lab %CVs.

Virus	Method B				Virus mean	Between lab %CV
	Lab 1	Lab 2	Lab 3	Lab 4		
IVR-116	46.62	54.46	46.72	44.67	**48.12**	**9.00**
NYMC X-157	49.23	50.46	47.31	42.81	**47.45**	**7.07**
NYMC X-161b	45.87	50.67	44.37	46.09	**46.75**	**5.82**
PR8	45.73	52.16	48.44	49.19	**48.88**	**5.41**
Lab Mean	**46.86**	**51.94**	**46.71**	**45.63**	**47.79 (overall)**	**5.91**

Values shown are the averages of at least 3 independent experiments.
Bold indicates means between viruses and/or labs, as well as CVs.

Table 3
Method A pooled CVs (within lab and within virus – based on replicate tests).

Method A						
Lab			Virus			
1	2	3	IVR-116	NYMC X-157	NYMC X-161b	PR8
5.46	4.72	13.55	5.93	9.38	9.11	3.50
7.02						

Table 4
Method B Pooled CVs (within lab and within virus – based on replicate tests).

Method B							
Lab				Virus			
1	2	3	4	IVR-116	NYMC X-157	NYMC X-161b	PR8
3.53	5.84	6.10	7.90	6.14	5.71	6.32	5.54
5.75							

account the range of variability between replicates in lab 3, there is no evidence to suggest that the variability between viruses is anything more than assay variation. However, the pooled within virus CVs are much lower (3.5%–9.4%) than the between lab CVs (10%–30% from Table 1), suggesting that the variability between labs for method A is greater than assay variation alone. This was confirmed by two-way analysis of variance where all labs were significantly different from all other labs ($p < 0.001$ in all cases).

For method B, all pooled CVs were less than 10% and were comparable with the between lab and between virus figures from Table 2 indicating that the %CVs from Table 2 are similar to assay variation. However, a two-way analysis of variance showed the mean for lab 2 to be higher than all other labs; although the difference in means was small, it was statistically significant ($p < 0.001$). No significant differences were found between any other labs ($p > 0.05$ in all cases).

From the data provided, both methods A and B give similar overall mean %HA results (44%, Table 1, and 48%HA, Table 2, respectively). Overall assay variation, as measured by the overall pooled %CV's was similar for both methods. The variability between viruses was low for both methods and comparable with between replicate variability, however method B showed improved agreement between labs compared to method A.

4. Conclusion

We have previously demonstrated that a modification of the SDS-PAGE method to include deglycosylation of samples before analysis improved the reproducibility of the quantitation of the HA of H5N1 viruses in our laboratory [8]. A study by Li et al. [10] also showed that the modified method led to very reproducible data for HA content (% HA) in pandemic H1N1 viruses. Here we have demonstrated that the new protocol for determination of HA content, which involves deglycosylation of the samples prior to running SDS-PAGE, improved the agreement between the laboratories participating in the study. The study involved 4 ERL laboratories assessing the HA content for a panel of seasonal influenza viruses using their current standard in-house method and the new prescribed method for deglycosylation. The overall results for percentage HA content, while displaying a trend towards slightly higher HA content values, were not statistically significantly changed by use of the modified method, which is a reflection of the robustness of the methods currently used; however, a move towards even closer agreement between the results generated is a significant improvement. This study was carried out using a small selection of seasonal influenza A virus samples. The level of glycosylation can vary (significantly) between different influenza viruses and so it may be found in the future that this method is even more useful for particularly problematic viruses. For example, some H5N1 strains have been shown previously [8] to have a significant problem of co-migration of proteins due to the level of glycosylation of the HA. It may be of value to continue the comparison of currently used methods alongside the deglycosylation protocol during the calibration of reference reagents over a number of influenza seasons to obtain more data and to fully assess the suitability of such a method for the calibration of reagents in the future. The deglycosylation step may need to be optimised for each new strain at the start of a season as we have seen some differences between viruses in the sensitivity to the PNGase F enzyme, with some viruses requiring longer periods of treatment, or more enzyme in the reaction (data not shown). In the future we can also investigate ways to improve agreement for the total protein determination, which is the other part of the collaborative process for calibration of potency reference reagents. There is potential to optimise this part of the assay as well as the HA quantitation procedure and so improve the reproducibility of calibration further. In the future it might be worth investigating the standardisation of SDS-PAGE gel consumables, equipment and protocols as well as standardisation of the quantitation procedure between the ERLs; however, as the present study shows, this is not needed urgently. Other physicochemical methods such as mass spectrometry can also be used to measure the absolute amount of a protein in a sample; ultimately a method such as this may be even more accurate. However, a lot of assay development and validation would be required before a new method like that could be employed, and a method like mass spectrometry requires more expertise and specific equipment, so it may be some time before it could be used routinely in all ERLs. Overall this study shows that the new method is more reproducible and thus has the potential to improve the calibration of influenza reference antigen reagents.

Acknowledgements

This work was funded in part by an MRC grant (number G0600509) awarded to Dr J.S. Robertson. We would like to thank Robert Newman for providing the panel of virus concentrates.

References

[1] Germann TC, Kadau K, Longini IM, Macken CA. Mitigation strategies for pandemic influenza in the United States. PNAS 2006;103:5935–40.
[2] Russell CA, Jones TC, Barr IG, Cox NJ, Garten RJ, Gregory V, et al. Influenza vaccine strain selection and recent studies on the global migration of seasonal influenza viruses. Vaccine 2008;26S:D31–4.
[3] Tosh PK, Jacobson RM, Poland GA. Influenza vaccines: from surveillance through production to protection. Mayo Clin Proc 2010;85(3):257–73.
[4] Orenstein WA, Schaffner W. Lessons Learned: Role of influenza vaccine production, distribution, supply and demand – What it means for the provider. Am J Med 2008;121:S22–7.
[5] Wood JM, Schild GC, Newman RM, Seagroatt V. An improved single-radial-immunodiffusion technique for the assay of influenza haemagglutinin antigen: application for the potency determinations of inactivated whole virus and subunit vaccines. J Biol Stand 1977;5:237–47.
[6] WHO. WHO Expert committee on Biological Standardization. Thirteenth report. Geneva: World Health Organisation; 1979. Annex 3 (WHO Technical Report Series, No. 638).
[7] Wood JM, Mumford JA, Dunleavy U, Seagroatt V, Newman RW, Thornton D, et al. Single radial immunodiffusion potency tests for inactivated equine influenza vaccines. In: Powell DG, editor. Equine infection disease V. Proc. Fifth International Conference. Kentucky: The University Press; 1988. p. 74–9.
[8] Harvey R, Wheeler JX, Wallis CL, Robertson JS, Engelhardt OG. Quantitation of haemagglutinin in H5N1 influenza viruses reveals low haemagglutinin content of vaccine virus NIBRG-14 (H5N1). Vaccine 2008;26:6550–4.
[9] Hsu JC. Multiple comparisons, Theory and methods. Chapman and Hall; 1996.
[10] Li C, Shao M, Cui X, Song Y, Li J, Yuan L, et al. Application of deglycosylation and electrophoresis to the quantification of influenza viral hemagglutinins facilitating the production of 2009 pandemic influenza (H1N1) vaccines at multiple manufacturing sites in China. Biologicals 2010;38:284–9.

Jpn. J. Infect. Dis., 65, 19-27, 2012

Original Article

Newly Established Monoclonal Antibodies for Immunological Detection of H5N1 Influenza Virus

Kazuo Ohnishi[1], Yoshimasa Takahashi[1], Naoko Kono[2], Noriko Nakajima[3], Fuminori Mizukoshi[1], Shuhei Misawa[4], Takuya Yamamoto[1], Yu-ya Mitsuki[1], Shu-ichi Fu[1], Nakami Hirayama[1], Masamichi Ohshima[1], Manabu Ato[1], Tsutomu Kageyama[2], Takato Odagiri[2], Masato Tashiro[2], Kazuo Kobayashi[1], Shigeyuki Itamura[2], and Yasuko Tsunetsugu-Yokota[1]*

[1]*Department of Immunology,* [2]*Influenza Virus Research Center, and*
[3]*Department of Pathology, National Institute of Infectious Diseases, Tokyo 162-8640; and*
[4]*Tsuruga Institute of Biotechnology, Toyobo, Co., Ltd., Fukui 914-8550, Japan*

(Received October 4, 2011. Accepted October 28, 2011)

SUMMARY: The H5N1 subtype of the highly pathogenic (HP) avian influenza virus has been recognized for its ability to cause serious pandemics among humans. In the present study, new monoclonal antibodies (mAbs) against viral proteins were established for the immunological detection of H5N1 influenza virus for research and diagnostic purposes. B-cell hybridomas were generated from mice that had been hyperimmunized with purified A/Vietnam/1194/2004 (NIBRG-14) virion that had been inactivated by UV-irradiation or formaldehyde. After screening over 4,000 hybridomas, eight H5N1-specific clones were selected. Six were specific for hemagglutinin (HA) and had in vitro neutralization activity. Of these, four were able to broadly detect all tested clades of the H5N1 strains. Five HA-specific mAbs detected denatured HA epitope(s) in Western blot analysis, and two detected HP influenza virus by immunofluorescence and immunohistochemistry. A highly sensitive antigen-capture sandwich ELISA system was established by combining mAbs with different specificities. In conclusion, these mAbs may be useful for rapid and specific diagnosis of H5N1 influenza. Therapeutically, they may have a role in antibody-based treatment of the disease.

INTRODUCTION

The highly pathogenic (HP) H5N1 avian influenza virus caused the first outbreak in humans in Hong Kong in 1997. This outbreak resulted in the infection of 18 people and resulted in six deaths (1,2). Thereafter, it was determined that H5N1 avian influenza virus was continuously circulated among geese in Southeastern China. Eventually, it spread to other Southeast Asian countries, where it severely damaged poultry farms (3,4). Subsequent H5N1 outbreaks in humans occurred in China and Vietnam in 2003 and in Indonesia in 2005. The most recent endemic has occurred in Egypt. According to a World Health Organization report, the H5N1 avian influenza virus had infected 565 people and resulted in 331 deaths by August 19, 2011 (5). Therefore, although sporadic, this fatal human infection is persistent and has the potential to cause serious future pandemics.

In humans, infection with HP H5N1 avian influenza virus causes high fever, coughing, shortness of breath, and radiological findings of pneumonia (6–8). In severe cases, rapidly progressive bilateral pneumonia develops, causing respiratory failure and may be responsible for the high mortality associated with this virus. de Jong et al. analyzed human cases of H5N1 infection and found that a high viral load and the resulting intense inflammatory response caused severe symptoms; furthermore, viral RNA was frequently detected in the rectum, blood, and nasopharynx (9). Thus, it is essential to detect HP influenza virus infection early and rapidly in order to provide early interventions that protect patients from devastating respiratory failure that arises from a high viral load. Additionally, early viral detection would facilitate rapid identification of infected patients and prevent unregulated contact with other people.

The present diagnostic standard for HP H5N1 influenza is the presence of the neutralization antibody. However, it takes more than 1 week for H5N1-specific antibodies to develop, and a well-equipped biosafety level 3 (BSL3) laboratory is required for the virus neutralization assay. A simpler method is the hemagglutination-inhibition assay using horse erythrocyte. This method has been widely performed on paired acute and convalescent sera from patients with HP H5N1 influenza virus infections. Although this method has acceptable sensitivity, its specificity has been questioned (7).

Isolating the virus from patient samples is the gold standard for diagnosing an infection; however, this is not always possible. For example, the method of sample preparation and preservation strongly influence the ability to isolate the virus. Moreover, a BSL3 laboratory is essential. At present, the most sensitive and rapid method for initial diagnosis of H5N1 virus infections is by conventional or real-time reverse-transcriptase polymerase chain reaction (RT-PCR). However, this proce-

*Corresponding author: Mailing address: Department of Immunology, National Institute of Infectious Diseases, Toyama 1-23-1, Shinjuku-ku, Tokyo 162-8640, Japan. Tel: +81-3-5285-1111, Fax: +81-5285-1150, E-mail: yyokota@nih.go.jp

dure requires expertise in molecular virology and expensive equipment and reagents. Moreover, because of its high sequence specificity, this approach could fail to identify mutant influenza viruses that continually evolve due to a high mutation rate (8).

For screening suspected H5N1 influenza virus in the field, the ideal approach would be to employ an immunology-based technique that detects viral antigens. Such a method is simple and rapid. However, its sensitivity and specificity depend highly on the antibodies used. Thus, an immunological assay that uses appropriate specific antibodies against H5N1 in combination with specific antibodies against other subtypes of influenza virus or viruses that cause febrile diseases would be useful for screening in areas with endemic influenza-like illness. While there are several rapid influenza virus diagnostic systems available for seasonal influenza (10), few exist for H5N1 influenza. Therefore, we have developed a simple and rapid diagnostic system with high sensitivity and specificity for H5N1 influenza virus.

Influenza virus belongs to the family *Orthomyxoviridae*; its genome consists of a negative-sense, single-stranded RNA with eight segments, each encoding structural and non-structural proteins (11). Influenza A viruses are classified into several subtypes based on the hemagglutinin (HA) and neuraminidase (NA) serotypes. In total, there are 16 HA and 9 NA serotypes. The H5N1 viruses are divided into clades 1 and 2 based on their HA genotypes. Clade 2 has been further subdivided into five sub-clades (12). Clade 1 viruses were predominant in Vietnam, Thailand, and Cambodia in the early phase of the 2004–2005 outbreak, whereas clade 2.1 viruses were endemic in Indonesia at that time (8). These two viruses are the major prototypes for the preparation of prepandemic H5N1 vaccines. We used inactivated purified clade 1 virion [A/Vietnam/1194/2004 (NIBRG-14)] as an immunizing antigen to establish mouse monoclonal antibodies (mAbs) specific for H5N1 influenza virus. Characterization of these mAbs revealed that they could detect H5N1 viruses when used in an immunofluorescence staining assay (IFA), Western blotting analysis, immunohistochemistry, and antigen-capture sandwich ELISA. In addition, the mAbs had significant in vitro neutralization activity against H5N1 viruses, and some broadly detected both clade 1 and 2 viruses.

MATERIALS AND METHODS

Viruses and cell culture: The NIBRG-14 (H5N1) virus, which possesses modified HA and NA genes derived from the A/Vietnam/1194/2004 strain on the backbone of six internal genes of A/Puerto Rico/8/34 (PR8), was provided by the National Institute for Biological Standards and Controls (NIBSC; Potters Bar, UK). A/Indonesia/05/2005 (Indo5/PR-8-RG2), A/Turkey/1/2005 (NIBRG-23), A/Anhui/01/2005 (Anhui01/PR8-RG5) were also obtained from NIBSC. All non-H5N1 strains were obtained from a stockpile of seed vaccines of the Influenza Virus Research Center of the National Institute of Infectious Diseases. The live virus was manipulated in a BSL2 laboratory. To produce and purify the virion, the NIBRG-14 and PR8 viruses were propagated in the allantoic cavity of 10-day-old embryonated hens' eggs and purified through a 10–50% discontinuous sucrose gradient by ultracentrifugation (13). The viruses were then resuspended in phosphate-buffered saline (PBS) and inactivated by ultraviolet (UV) irradiation or by treatment with 0.05% formalin at 4°C for 2 weeks. These preparations were served as the inactivated H5N1 virus fraction. These conditions have been previously shown to completely inactivate H5N1 viruses.

Production of mAbs: Nine-week-old female BALB/c mice (Japan SLC, Shizuoka, Japan) were immunized subcutaneously with 20 μg of UV- or formaldehyde-inactivated NIBRG-14 (H5N1) virus using Freund's Complete Adjuvant (Sigma, St. Louis, Mo., USA). Two weeks later, the mice were boosted with a subcutaneous injection of 5 μg of the inactivated virus emulsified with Freund's Incomplete Adjuvant (Sigma). Three days after the boost, sera from the mice were tested by ELISA to determine the antibody titer against the NIBRG-14 virus. The three mice with the highest antibody titers were given an additional boost 14 days after the first boost by intravenous injection of 5 μg of the inactivated virus. Three days later, the spleens of these three mice were excised, and the spleen cells were fused with Sp2/O-Ag14 myeloma cells using the polyethylene glycol method of Kozbor and Roder (14). The fused cells were cultured on twenty 96-well plates and selected with hypoxiantine-aminopterin-thymidine (HAT) medium. The first screening was conducted by ELISA using formalin-inactivated purified NIBRG-14 (H5N1) and PR-8 (H1N1) virions, which were lysed with 1% Triton X100. The lysates (1 mg/ml) were diluted 2,000-fold with ELISA-coating buffer (50 mM sodium bicarbonate, pH 9.6), and the ELISA plates (Dynatech, Chantily, Va., USA) were coated at 4°C overnight. After blocking with 1% ovalbumin in PBS-Tween (10 mM phosphate buffer, 140 mM NaCl, 0.05% Tween 20, pH 7.5) for 1 h, the culture supernatants of the HAT-selected hybridomas were added and incubated for 1 h. After washing with PBS-Tween, the bound antibodies were detected using alkaline phosphatase-conjugated anti-mouse IgG (1:2,000; Zymed, South San Francisco, Calif., USA) and *p*-nitrophenyl phosphate, which served as a substrate. In this first screening, hybridomas that reacted to the H5N1 virus (NIBRG-14) but not to the H1N1 virus (PR-8) were selected.

Baculoviral expression of recombinant HA and NA: Recombinant HA (rHA) and NA (rNA) proteins were produced as previously described (13). Briefly, the HA- and NA-coding genes of NIBRG-14 were amplified by PCR to attach a 6x-His tag to the C terminus of HA and to the N terminus of NA. The amplified DNAs were then cloned into pBacPAK8 (Clontech, Mountain View, Calif., USA) and transfected into Sf-21 (*Spodoptera frugiperda*) insect cells. Recombinant baculoviruses containing the rHA and rNA genes were isolated were used to infect Sf-21 cells. The recombinant proteins tagged with 6x-His were purified with TALON columns (Clontech) according to the manufacturer's protocol.

Neutralization assay: For the neutralization assay, 100 $TCID_{50}$ of H5N1 virus, a standard tissue culture infectious dose for such assays, was incubated for 30 min at 37°C in the presence or absence of the purified mAbs, which had been serially diluted twofold. The viruses

were then added to MDCK cell cultures that had been grown to confluence in a 96-well microtiter plate. The virus strains used were A/Vietnam/1194/2004 (NIBRG-14) (H5N1) (clade 1), A/Indonesia/05/2005 (Ind05/PR8-RG2) (H5N1) (clade 2.1), A/Turkey/1/2005 (NIBRG-23) (H5N1) (clade 2.2), and A/Anhui/01/2005 (Anhui01/PR8-RG5) (H5N1) (clade 2.3). After 3–5 days, the cells were fixed with 10% formaldehyde and stained with crystal violet to visualize the cytopathic effects induced by the virus (15). Neutralization antibody titers were expressed as the minimum concentration of purified immunoglobulin that inhibited a cytopathic effect.

Western blot analysis: UV-inactivated purified H5N1 virus (0.5 μg/lane) was loaded on SDS-PAGE gels under reducing conditions. The proteins were then transferred to a PVDF membrane (Genetics, Tokyo, Japan). After blocking with BlockAce reagent (Snow Brand Milk Products Co., Tokyo, Japan), the membranes were detected with the mAbs or diluted sera (1:1,000) that had been obtained from mice immunized with UV-irradiated H5N1 virus. After washing, the membrane was reacted with the peroxidase-conjugated $F(ab')_2$ fragment of anti-mouse IgG (H + L) (1:20,000; Jackson ImmunoResearch, West Grove, Pa., USA), and the bands were visualized on X-ray film (Kodak, Rochester, N.Y., USA) with chemiluminescent reagents (Amersham Biosciences, Piscataway, N.J., USA).

Purification and biotinylation of mAbs: Hybridomas were grown in Hybridoma-SFM medium (Invitrogen, Carlsbad, Calif., USA) supplemented with recombinant IL-6, penicillin (100 U/mL), and streptomycin (100 μg/mL) (16). The culture supernatants were harvested, and 1/100 volume of 1 M Tris-HCl (pH 7.4) and 1/500 volume of 10% NaN_3 were applied directly on a Protein G-Sepharose 6B column (Amersham Biosciences). The column was washed with PBS and eluted with glycine/HCl (pH 2.8). After measuring the OD_{280} of the fractions, the protein-containing fractions were pooled, and an equal volume of saturated $(NH_4)_2SO_4$ was added. The precipitated proteins were dissolved in PBS, dialyzed against PBS, and stored at −20°C. The purified antibodies were biotinylated with sulfo-NHS-LC-biotin (Pierce, Rockford, Ill., USA) according to the manufacturer's protocol.

Antigen-capture ELISA: The purified antigen-capturing mAb was immobilized on a microplate (Immulon 2; Dynatech) by incubating 4 μg/mL of the mAb in 50 mM sodium bicarbonate buffer (pH 8.6) at 4°C overnight. The microplate was blocked with 1% BSA, washed with PBS-Tween, and reacted with serial dilutions of UV-inactivated purified H5N1 virus for 1 h at room temperature. After washing with PBS-Tween, biotinylated probing mAb (0.1 μg/mL) was added to the wells for 1 h at room temperature. After washing, horseradish peroxidase (HRP)-labeled streptavidin (Zymed) was added to the wells for 1 h at room temperature. After washing, 0.4 mg/mL *o*-phenylenediamine (OPD Sigma P-8412) in OPD Buffer (0.05 M citrate-phosphate buffer pH 5.0, 0.04% H_2O_2) or TMB(+) substrate (DAKO, Kyoto, Japan) was added. The reaction was stopped by adding 2N H_2SO_4, and the OD_{490} or OD_{450} was measured using a multi-well plate reader (Flow Laboratories Inc., Inglewood, Calif., USA).

Immunohistochemistry: Lung tissues were harvested from mice infected with A/Vietnam/1194/2004 (NIBRG-14) or A/HongKong/483/97 (HK483). In addition, autopsied lung tissues of patients infected with influenza virus (H1N1 or 2009 H1N1pdm) were used. Formaldehyde- or formalin-fixed paraffin-embedded lung tissue sections were deparaffinized with xylene and graded ethanol and then autoclaved in 0.1 M citrate-buffer (pH 6.0) at 121°C for 10 min to retrieve the antigens. Endogenous peroxidase was inactivated with 0.3% hydrogen peroxide for 30 min at room temperature. After blocking with M.O.M. blocking reagent (Vector laboratories, Burlingame, Calif., USA) or 5% goat serum, the sections were incubated with each of the mouse mAbs or rabbit polyclonal antibody against type A influenza nucleoprotein at 4°C overnight. After washing off the excess antibodies, the sections were incubated with HRP-labeled anti-mouse IgG followed by tyramide signal amplification system (Biotin-free catalyzed amplification system, CSAII; DAKO) or biotinylated anti-rabbit IgG followed by streptavidin/HRP (LSAB kit; DAKO). The labeled peroxidase activity was detected using diaminobenzidine (DAB; Dojin, Kumamoto, Japan) in 0.015% hydrogen peroxide/0.05 M Tris-HCl (pH 7.6). The sections were counterstained with hematoxylin.

RESULTS

Generation of H5N1-specific mAbs: To establish hybridomas that secrete mAbs specific for the H5N1 virus, BALB/c mice were immunized with the whole virion fraction of purified A/Vietnam/1194/2004 (NIBRG-14) virus. The virus had been inactivated by conventional formaldehyde-fixation or by UV-irradiation to avoid possible changes in antigenicity caused by aldehyde fixation. A standard immunization protocol was used, where mice were boosted twice at 2-week intervals with antigen emulsified first in Freund's Complete Adjuvant and then in Freund's Incomplete Adjuvant. Three days after the final boost, a cell suspension was prepared from the spleens of three immunized mice and fused with SP-2/O myeloma using a polyethylene-glycol method. The fused cells were then selected with HAT (14). Hybridoma screening yielded eight hybridoma clones that reacted to NIBRG-14 lysate but not PR-8 lysate in ELISA (Table 1). Of these clones, seven were from mice immunized with UV-inactivated virion, and one was from mice immunized with formaldehyde-inactivated virion. Six clones (Niid_H5A, Niid_H5B, Niid_H5C, Niid_H5D, Niid_H5E, and Niid_H5F) reacted to rHA protein from a H5N1 virus (recHA_H5N1), while one clone (Niid_N1A) reacted to rNA protein from a H5N1 virus (recNA_H5N1). The remaining clone (Niid_150KA) did not react to either recHA_H5N1 or recNA_H5N1 by ELISA but did react to a 150-kDa molecule on Western blot analysis (described below). Interestingly, seven of the eight clones were from the mice immunized with UV-inactivated virus. The eight hybridomas were successfully cloned by a repeated limiting-dilution method and adapted to a serum-free hybridoma culture medium. The purified antibodies from each clone were biotinylated and used for further experiments.

Table 1. Summary of the eight H5N1-specific mAbs generated in this study

Clone name	Old name	Ig-subclass	ELISA				Western blot	IFA	Histology	Neutralization (μg/mL)	Hemagglutination inhibition
			H5N1_ NIBRG-14	H1N1_ PR-8	recHA_ H5N1	recNA_ H5N1					
Niid_H5A[1)]	YH-1A1	IgG2a	+++	−	+	−	57 kDa	++		1.5 (Clade-dep)	−
Niid_H5B[1)]	YH-2F11	IgG2a	+++	−	+++	−	57 kDa			25	+
Niid_H5C[1)]	OM-A	IgG2a	+++	−	++	−	57 kDa		+(mo/hu)	12	
Niid_H5D[1)]	OM-B	IgG2a	+++	−	++	−	57 kDa		+(mo)	12	
Niid_H5E[1)]	OM-C	IgG2a	+++	−	++	−	57 kDa			12 (Clade-dep)	
Niid_H5F	AY-2C2	IgG1	+++	−	++	−	ND	++		6	−
Niid_N1A[1)]	YH-2D3	IgG2a	+++	−	−	+	ND	++			
Niid_150KA[1)]	OM-D	IgG1	+++	−	−	−	150 kDa	++			−

[1)]: Clones derived from mice immunized with UV-inactivated virus. The remaining clone is derived from a mouse immunized with formaldehyde-inactivated virus.

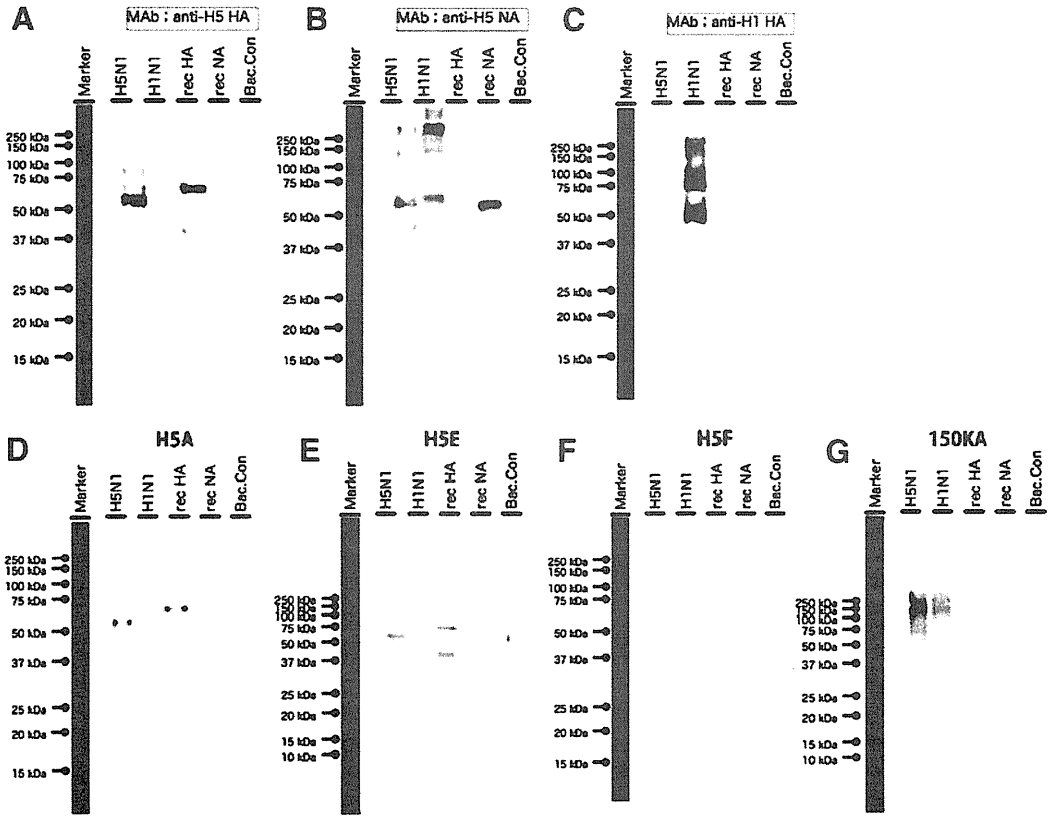

Fig. 1. Detection of influenza virus proteins in Western-blot analysis. Purified influenza virus proteins (0.5 μg/lane) were subjected to SDS-PAGE under reducing conditions. After blotting on a PVDF membrane, the proteins were detected by incubation with the eight monoclonal antibodies (mAbs), followed by incubation with the peroxidase-labeled $F(ab')_2$ fragment of donkey anti-mouse IgG. The mAbs were then visualized by chemiluminescent reaction. A, authentic anti-H5_hemagglutinin mAb; B, authentic anti-H5_neuraminidase mAb; C, authentic anti-H1_hemagglutinin mAb; D, Niid_H5A; E, Niid_H5E; F, Niid_H5F; G, Niid_150KA. The molecular weight markers are shown on the left.

Western blot analyses with the mAbs: Five mAbs (Niid_H5A, Niid_H5B, Niid_H5C, Niid_H5D, Niid_H5E) detected the 57-kDa H5_H1 protein by Western blot analysis, which suggests that the antibodies detected the linear epitope(s) of a HA1 fragment of H5_HA (Table 1 and Fig. 1). These antibodies also detected the 60-kDa recombinant H5-HA containing the His-tag. One of these clones, Niid_H5E, detected a 40-kDa subfragment of recombinant HA1, which suggests that the antigenic footprint detected by the mAb differs from that of the other four clones (Fig. 1). Niid-H5F, which reacted strongly to NIBRG-14 and rHA (H5) in ELISA, did not react to any proteins by Western blot analysis, presumably because the mAb detects a conformational epitope of H5-HA. The remaining clone, Niid_150KA, detected an unknown high molecular weight protein of approximately 150 kDa.

IFA with mAbs: Upon IFA, the HA-specific mAbs Niid-H5A and Niid_H5F, the NA-specific mAb Niid-N1A, and the Niid_150KA mAb that detects an

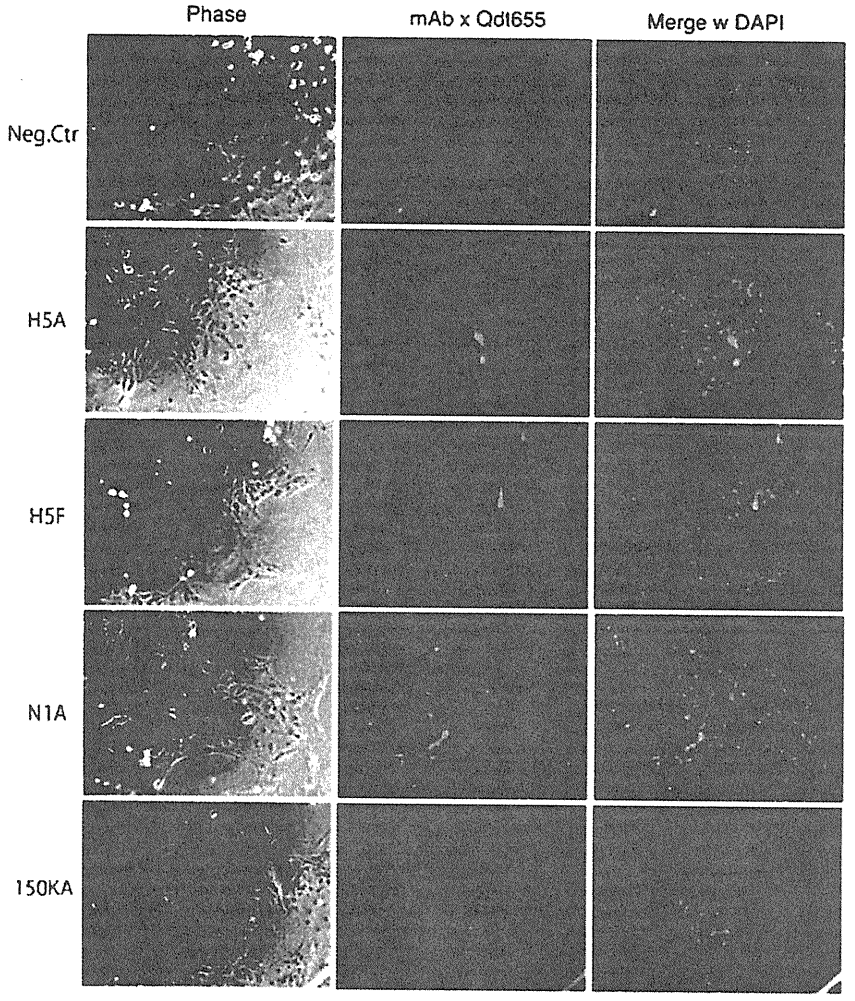

Fig. 2. Fluorescent immunostaining of H5N1 virus-infected MDCK cells with monoclonal antibodies (mAbs). Paraformaldehyde-fixed, H5N1 virus-infected MDCK cells were permeabilized by TBS-Tween and incubated with biotinylated mAbs. The mAbs were detected with Qdot655-conjugated streptavidin (red). Shown are representative staining patterns with Niid_H5A, Niid_H5F, Niid_N1A, and Niid_150KA. The negative control staining without mAb is shown on top. The nuclei were counterstained with DAPI (blue).

unknown 150-kDa protein bound to NIBRG-14-infected MDCK cells (Fig. 2). With the exception of Niid_H5F, these mAbs detected both the perinuclear region and the cell surface of NIBRG-14-infected MDCK cells. Niid_H5F did not detect the perinuclear region (presumably the Golgi body), which suggests that the antigenic footprint detected by this mAb differs from those of the other mAbs.

Immunohistochemistry: The Niid_H5C and Niid_H5D mAbs detected influenza virus antigens in the epithelial cells of the bronchioles and alveoli of 4% formaldehyde-fixed, paraffin-embedded lung tissue sections from mice infected with A/Vietnam/1194/2004 (NIBRG-14) (Fig. 3a). However, none of the mAbs detected influenza virus antigen in lung tissue sections from mice infected with A/HongKong/483/97 (HK483) (Fig. 3). In contrast, a polyclonal antibody against type A influenza nucleoprotein detected type A influenza virus nucleoprotein in the tissue sections from both the NIBRG-14- and HK483-infected mice (Fig. 3b, d). Thus, Niid_H5C and Niid_H5D specifically detected the HA antigen of A/Vietnam/1194/2004 (NIBRG-14). The specificity of these mAbs was then examined by using autopsied lung tissue sections from patients infected with seasonal influenza virus (H1N1) or 2009 pandemic influenza virus (2009H1N1pdm). Niid_H5C did not exhibit any crossreactivity, but the Niid_H5D mAb did show non-specific staining with the human lung section. Two other mAbs, Niid_H5B and Niid_N1A, were also subjected to such immunohistochemical analysis but did not show any reaction.

Neutralization assay with mAbs: The ability of the mAbs to neutralize several H5N1 influenza strains was then tested (Table 2). The four purified H5N1 virus strains, NIBRG-14, Indo-RG2, NIBRG-23, and Anhui-RG5, were diluted to 2–3 $\times$ 10^2 $TCID_{50}$/0.05 mL (Table 2, lower panel) and incubated with titrated amounts of anti-H5_HA mAbs. The remaining infectivity was then noted (Table 2, upper panel). Niid_H5A most potently neutralized the NIBRG-14 strain; it completely neutralized influenza virus infectivity at a concentration of 78 ng/mL. However, Niid_H5A was less potent in neutralizing the Indo-RG2 and Anhui-RG5 strains, which indicates that the neutralizing ability of this mAb was clade-dependent. In contrast, Niid_H5F and Niid_H5D exhibited relatively broad neutralizing abilities, since they neutralized all of the strains that were tested. Niid_H5C and Niid_H5E also showed characteristic clade-

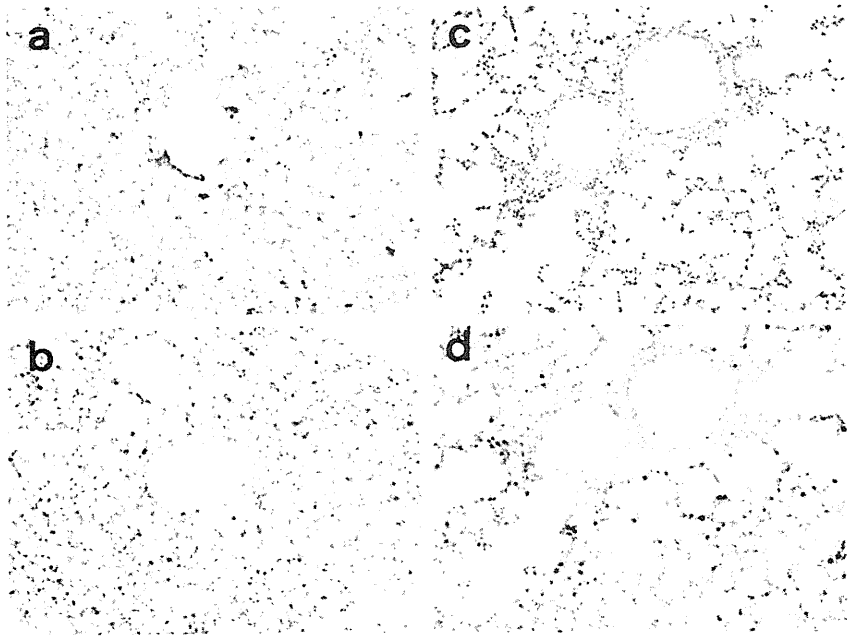

Fig. 3. Immunohistochemical analyses of lung sections from mice infected with A/Vietnam/1194/2004 (NIBRG-14) or A/HongKong/483/97 (HK483) virus. (a, b) Influenza virus antigens were detected in the epithelial cells of the bronchioles and alveoli of the mouse infected with A/Vietnam/1194/2004 (NIBRG-14) by the Niid_H5C clone (a) and polyclonal antibody against type A influenza nucleoprotein (b). (c, d) Virus antigens were not detected in the lung tissue section of the mouse infected with A/HongKong/483/97 (HK483) when Niid_H5C was used (c). However, virus antigens were detected in this section when a polyclonal antibody against type A influenza nucleoprotein was employed (d).

Table 2. Neutralizing ability of the eight mAbs generated in this study

Clone	Neutralizing antibody titer (ng/mL)			
	NIBRG-14 (clade 1)	Indo-RG2 (clade 2.1)	NIBRG-23 (clade 2.2)	Anhui-RG5 (clade 2.3)
Niid_H5A	78	>10,000	625	>10,000
Niid_H5C	625	625	313	>10,000
Niid_H5D	625	625	313	5,000
Niid_H5E	625	>10,000	>10,000	>10,000
Niid_H5F	313	313	156	2,500

Test no.	Virus infection index (Log_{10} $TCID_{50}$/0.05 mL)			
	NIBRG-14	Indo-RG2	NIBRG-23	Anhui-RG5
1	2.5	3.1	2.4	2.1
2	2.0	NT	2.0	2.4

The in vitro neutralization assay examined the ability of the mAbs to neutralize H5N1 virus infection of cultured MDCK cells. Briefly, purified H5N1 virus was diluted to 2–3 × 10^2 $TCID_{50}$/0.05 mL (the quantities are shown in the lower table) and incubated with serially-titrated purified mAbs for 1 h at 37°C. The samples were then placed into 96-well plates in which MDCK cells had been grown to 90% confluence. After 48 h, the cytotoxicity of the mAb-treated viruses was visualized by staining the cells with crystal violet.
NT, not tested.

dependency, suggesting that the epitopes of these mAbs differ. Interestingly, the mAbs were least able to neutralize Anhui-RG5. This may reflect the genetic distance between Anhui-RG5 (clade 2.3) and NIBRG-14 (clade 1).

Antigen-capture ELISA: To quantitatively detect H5N1 virus, we constructed a sandwich ELISA-based virus antigen-capture detection system. Preliminary experiments tested all combinations of two mAbs from the eight mAbs; Niid_H5F had the highest detection sensitivity for purified H5N1 virion and reacted broadly to the H5_HA of viruses belonging to clades 1, 2.1, 2.2, and 2.3. Therefore, Niid_H5F was selected as the antigen-capturing mAb. The antigen-capture ELISA was constructed by immobilizing Niid_H5F (and/or Niid_H5C) on the ELISA plate and using biotinylated Niid_H5D as the detection mAb, since this combination gave the best results (data not shown). Since the eight mAbs

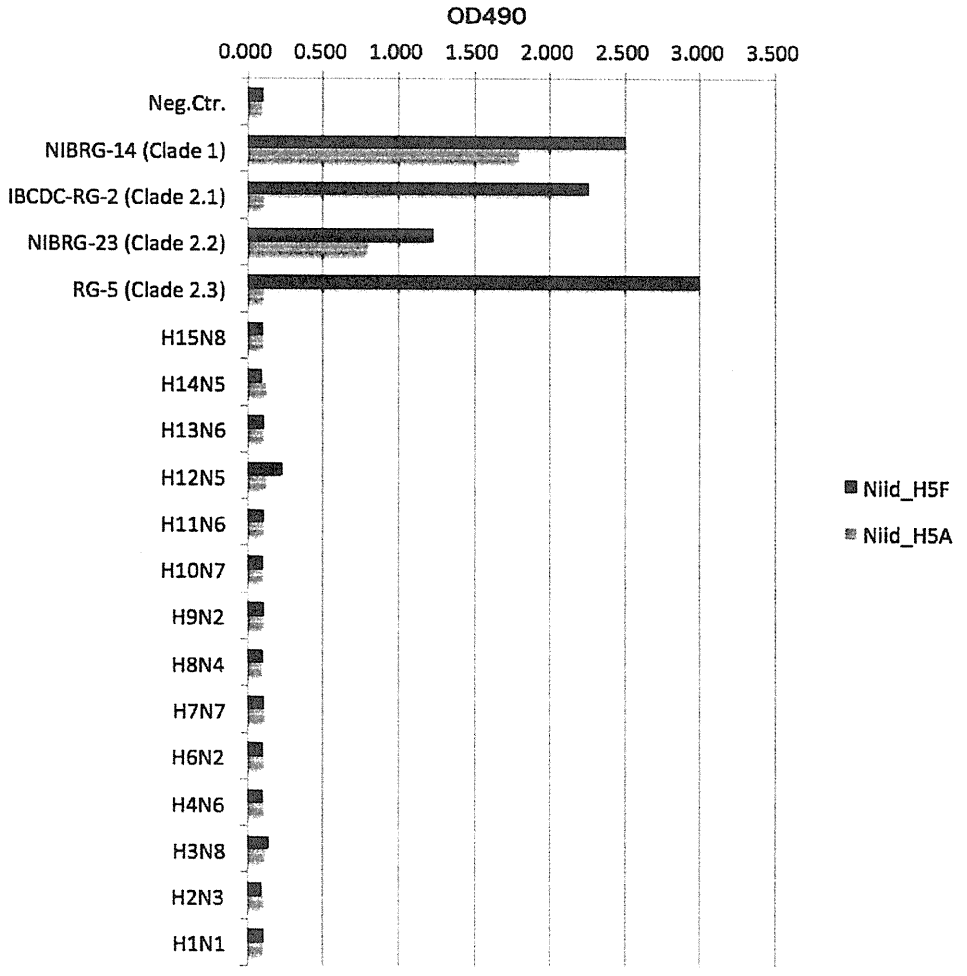

Fig. 4. ELISA reactivity of the Niid_H5A and Niid_H5F monoclonal antibodies (mAbs) to various influenza virus strains. Different influenza virus strains were immobilized on 96-well plates and incubated with biotinylated Niid_H5A or Niid_H5F mAbs followed by peroxidase-labeled streptavidin. The binding of the mAbs was then quantitated by a colorimetric assay using TMB as a substrate.

were originally raised against the H5N1 virus strain A/Vietnam/1194/2004 (NIBRG-14), the validity of this system with other strains of H5N1 virus was also examined. As shown in Fig. 4, this system could detect the A/Indonesia/05/2005 (Indo5/PR-8-RG2), A/Turkey/1/2005 (NIBRG-23), and A/Anhui/01/2005 (Anhui01/PR8-RG5) strains but none of the non-H5N1 strains. The sandwich ELISA could detect H5N1 virus protein at concentrations as low as 50 ng/mL HA, namely, >3 SD of negative samples (Fig. 5).

DISCUSSION

In the present study, mAbs against H5N1 influenza virus were established. These mAbs could detect the virus when used in Western blot analyses, IFA, immunohistochemical analyses, neutralization assays, and antigen-capture ELISA. The characteristics of the mAbs are summarized in Table 1.

Of the eight mAb clones that reacted to H5N1 virus in ELISAs, six reacted to rHA. Only one clone reacted to NA protein. Another clone detected an unknown 150-kDa molecule upon Western blot analysis. A hybridoma that secreted a mAb that could detecte the nuclear protein or other protein components of H5N1 virus was not detected, presumably because the first screening step identified H5 specificity. These results indicate that the HA protein is a dominant target in the antibody response of HA-subtype specificity, as suggested by other studies (17,18). There is accumulating evidence that the influenza strain-specific epitopes are often localized on the HA1 region, whereas the epitopes that are conserved among various strains are localized on the HA2 region (19–22). It has been reported that the immune response elicited by H1N1pdm yields a high frequency of HA2-specific mAbs (23,24). In the present study, none of the established clones detected the HA2 fragment of H5HA, presumably because this study focused on H5-specific clones.

The mAbs isolated in the present study were assessed for their ability to detect H5N1 virus-infected MDCK cells in IFA. Indeed, the anti-HA and anti-NA mAbs detected the cytoplasmic Golgi-rich region and the cell surface membrane. This reflects the common assembly process of influenza virus (25).

In general, a single diagnostic test is not reliable because of the potential for false positives and negatives. Considering the restricted availability of RNA detection systems (26,27), serological screening systems other than those that detect antibodies are currently being ex-